J Mater Sci

Review

Recent trends in graphene materials synthesized by CVD with various carbon precursors

Muhammad Izhar Kairi[1], Mehrnoush Khavarian[1], Suriani Abu Bakar[2], Brigitte Vigolo[3,*], and Abdul Rahman Mohamed[1]

[1] *School of Chemical Engineering, Engineering Campus, Universiti Sains Malaysia, 14300 Nibong Tebal, Seberang Perai Selatan, Pulau Pinang, Malaysia*

[2] *Nanotechnology Research Centre, Faculty of Science and Mathematics, Universiti Pendidikan Sultan Idris, 35900 Tanjung Malim, Perak, Malaysia*

[3] *Institut Jean Lamour, CNRS-Université de Lorraine, BP 70239, 54506 Vandceuvre-lés-Nancy, France*

Received: 19 July 2017
Accepted: 9 October 2017

ABSTRACT

Graphene is a single layer of carbon atoms arranged in an sp^2-hybridized structure with properties far superior compared to other materials. Research and development in graphene synthesis have been rapidly growing the past few years, especially using chemical vapor deposition (CVD) over various types of carbon precursor. The nature and the type of carbon precursor is one important parameter of growth by CVD, especially for graphene production, since they can dramatically impact graphene growth yield and rate. However, effects of the used carbon precursor on graphene growth mechanisms are rarely discussed. In the course of large-scale and low-cost graphene preparation, this review on the recent trends regarding the utilization of diverse carbon precursors used to synthesize graphene via the CVD method is of great interest for development of improved or alternative synthesis methods. The details and the mechanisms involved in graphene synthesis using carbon precursors in the form of gaseous, liquids and solids are compared, analyzed and discussed thoroughly. In this review, we present a thorough overview on the impact and mechanisms of carbon precursors in achieving high-quality graphene with competitive edge in the near future.

Introduction

The unique properties of graphene have triggered a sudden drive of graphene researches all over the world. Graphene is expected to be the next generation of two-dimensional materials having the potential to enhance current technology and create a new one in the near future. Graphene is a thermodynamically stable species of pure carbon atoms bonded in a single sheet with hexagonal sp^2 structure [1]. It represents the base structure of carbon nanotubes (CNTs), graphite and fullerenes. Electron

Address correspondence to E-mail: Brigitte.Vigolo@univ-lorraine.fr

DOI 10.1007/s10853-017-1694-1

Published online: 20 October 2017

configuration of the carbon atoms is the key factor for the incredible properties of graphene such as its high mechanical strength [2, 3], high surface area [4, 5], extraordinary thermal conductivity [6, 7] and ultra-high elasticity [8]. The linear band structure of graphene is also located near the K-point that makes monolayer graphene 97% optically transparent [9, 10]. Due to its outstanding properties, graphene has an immense potential in many applications. Even if properties of graphene depend on its structure and form [11, 12] and the intended applications depend on graphene characteristics, its potential to improve performances in numerous materials and processes is widely recognized. Among the numerous applications targeted, graphene could be used as transparent conducting electrodes [13], fillers in reinforced polymer nanocomposites [14–16], super-capacitors [17–19], lithium ion batteries [20–22], fuel cells [23, 24], solar cells [25], photo-catalysis [26], biosensors [27], chemical sensors [28], purification of water [29] and optoelectronics [30, 31]. To face the demand for both fundamental studies and developments for its practical utilization, development of large-scale synthesis methods has never been more vital [32, 33].

Since the discovery of graphene through highly oriented pyrolytic graphite (HOPG) mechanical exfoliation [34, 35], a number of alternative methods of graphene synthesis have been developed. Wet chemical exfoliation is one of the most widely used techniques to prepare graphene nowadays, but it does have some drawbacks [36] including numerous lattice defects, multiple grain boundaries and oxidative traps, which increases its electrical resistance [37]. Other methods to synthesize graphene include intercalation [38], epitaxial growth from silicon carbide (SiC) [39], chemical vapor deposition (CVD) [40] and plasma and flash pyrolysis of solvothermal materials [41]. Among the aforementioned techniques, the growth of graphene by CVD on metal catalysts or semiconductor catalysts has been considered as the most promising technique because of its simple process and the capability of achieving large-area graphene with high crystalline quality [42, 43]. CVD is the dominant manufacturing route for many other nanomaterials such as CNTs [44] since it enables not only bulk production but also direct device integration. This bottom-up approach involves a carbon precursor being able to dissociate within a metal substrate, and a solubilization–segregation phenomenon leads to graphene formation. The involved mechanisms depend on the transition metals used [34, 45]. Generally, two types of mechanism are reported in graphene synthesis by CVD on transition metals: bulk-mediated and surface-mediated mechanism. For instance, Cu induces a surface-mediated growth mechanism which allows mastering the number of graphene layers as compared to many other transition metals [46, 47]. A bulk-mediated growth mechanism has been proposed for transition metals such as Ru, Ir and Ni [48]. The growth mechanism is closely related to carbon solubility from the precursor in the metal substrate at the operating CVD conditions, especially reaction temperature. This is the reason why aside from the metal substrate, the influence of the nature and the state of the carbon precursor used cannot be neglected since it certainly plays a major role in graphene CVD synthesis and growth mechanisms. There have been many published papers and reviews regarding the different mechanisms of catalysis of graphene synthesized by a transition metal [34, 45]. However, there is a lack of analysis and discussion regarding the possible mechanisms of carbon precursors for graphene synthesis via the CVD method.

In this review, the recent trends reported on investigation of carbon precursor effects on graphene synthesis by CVD are reviewed. This review will also propose a new mode of growth mechanism based on the chemical structure of the carbon precursor utilized. Until now, the two principal growth mechanisms for large-area graphene were surface-mediated and bulk-mediated mechanism depending on the transition metal used for the reaction. In this review, she shows that the catalyst nature and the operating conditions cannot explain alone the observed graphene growth. The used graphene precursor is a parameter that has not to be neglected to master graphene growth and its characteristics. For example, Jang et al. [49] group was able to grow monolayer graphene by using benzene as the precursor via CVD but at 300 °C with Cu as the metal catalyst. Standard CVD using methane as the carbon precursor and Cu as the metal catalyst would typically require temperature of around 1000 °C [50–52]. Why did the graphene growth temperature become so low while using benzene as precursor? This phenomenon will be explained in this review through the introduction of new growth mechanisms based on the carbon precursor used. From our observations and investigations, we found that the reported growth

mechanisms are appearing to be highly dependent on the chemical structure of the used carbon precursor.

The present review is organized into four parts. The first part deals with the different CVD setups for graphene synthesis from carbon precursors in the form of gaseous, liquid and solid. The second part retraces and analyses the various kinds of carbon precursors that have been investigated and published in internationally recognized journals. The third part elaborates and discusses the main themes reviewed and the mechanisms involved for each family of carbon precursors and their impact on the graphene properties. Lastly, some prospects of the covered aspects will be given.

Chemical vapor deposition

In 2009, it was the first time that CVD growth of monolayer graphene films was realized by using polycrystalline Cu foil as substrate [53]. CVD was recognized as a proficient method for graphene synthesis, and since then, there have been a lot of studies and experimentations aiming at further improving the process.

Cu as catalyst has many advantages compared to other transition metals including ease of transfer, economical cost and good control of number of layers. Growth mechanism by Cu has been proven to be a surface adsorption-mediated process [46, 54, 55]. The used carbon precursor can be, a priori, in the form of gas, liquid or solid. However, it always needs to be in the form of gas as it reaches the metal catalyst surface. The most widely used gaseous carbon precursors are hydrocarbons such as methane (CH_4) and acetylene (C_2H_2). The mechanism of graphene synthesis by Cu can be divided into three stages. At first stage, the carbon precursor molecules collide on the metal substrate surface. They can either adsorb on the surface, scatter back to the bulk gas phase or directly progress to the next stage of the reaction process. At second stage, the carbon precursor molecules dehydrogenate, partially dehydrogenate or remove non-carbon elements so that it can form active carbon species. Lastly, during third stage, these active species coalesce, nucleate and grow into graphene islands on top of the metal substrate [56]. These graphene islands enlarge until full coverage. If the used carbon precursor is under the form of liquid or solid, a supplementary stage precedes the collision phenomenon.

Numerous CVD setups have been successfully developed to synthesize graphene, especially from gaseous carbon precursors. The CVD methods used for liquid and solid precursors as feedstocks are less common. Figure 1 illustrates the main CVD setups used by researchers for liquid and solid precursors to grow graphene. All the setups have their own advantages and drawbacks depending on the used starting reactants and materials. For liquid precursors with elevated boiling point that do not readily evaporate like ethanol, an external source of heating is required to vaporize the precursor. The common procedure consists in heating up the catalyst until it reaches the desired reaction temperature; then, the region with the liquid precursor is heated above its boiling point. A flow of N_2 and H_2 carries the gaseous precursor to the metal substrate location for graphene growth. The common method involves a two-furnace setup which has also been extensively used for CNTs [57]. Some research groups have also used bubbling setup [58] and heating tape [56] to heat and convert the liquid precursor into gas. It is vital that the pathway from the external heating point to the heated catalyst zone is above the boiling point of the liquid precursor. Otherwise, the vaporized precursor might return to its original form and deposit onto the hot quartz tube. This represents an additional lead time as the contaminated quartz tube will need to be cleaned before a new experimental run can be performed. A magnetic boat setup can also be used for this particular purpose [59]. The magnetic boat carrying the solid or liquid precursor is initially placed at the front end of a long quartz tube with the metal catalyst in the furnace heating region. The furnace is then heated to the desired reaction temperature. Once the desired temperature is reached, the magnetic boat is moved closer to the furnace heating region using a magnet. The distance between the precursor and catalyst must be within the uniform heating zone of the catalyst. Aside from the CVD bubbling setup, similar setup can be performed for a solid precursor. For example, the two-furnace setup has been used multiple times to produce graphene from camphor [60, 61]. The total energy needed in CVD differs on the type of precursor used for the whole process [62, 63].

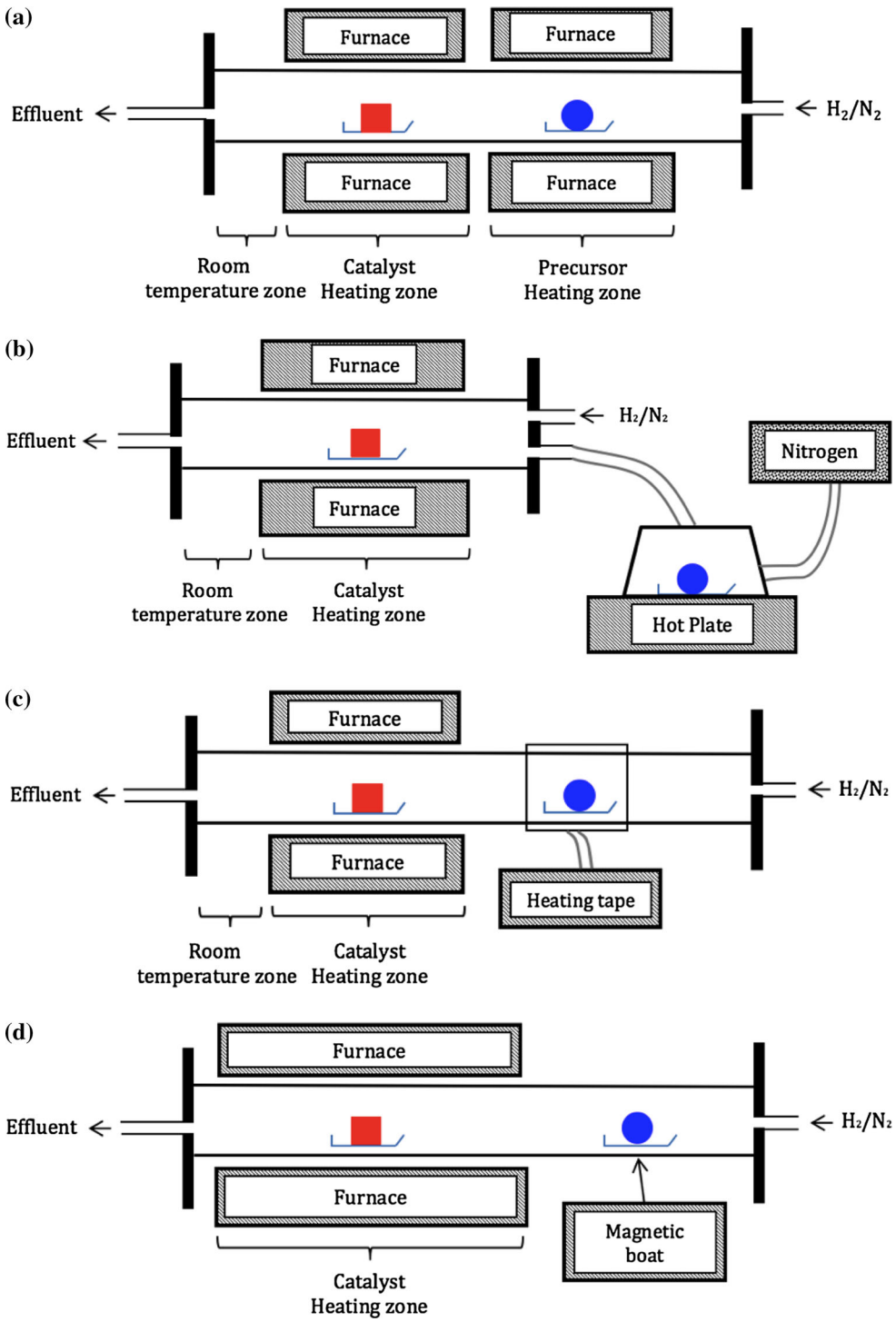

Figure 1 Chemical vapor deposition setups: **a** two-furnace; **b** bubbling; **c** heating tape; **d** magnetic boat. Square = catalyst; circle = precursor.

Gaseous carbon precursors

Methane (CH_4), acetylene (C_2H_2) and ethylene (C_2H_4) represent the typical gaseous carbon precursors used for graphene CVD synthesis. Methane has been the primary source of carbon for graphene synthesis by CVD for the last decade. Its strong C–H bonds make methane alone poorly reactive and insusceptible from

undergoing chemical reaction. With the addition of suitable catalyst, methane is a reliable carbon source for graphene growth [50, 64]. Normally, thermal CVD method using methane requires reaction temperature around 1000 °C to produce high-quality graphene on metal substrates [53, 65]. However, significant progress in decreasing the reaction temperature could be achieved by means of radio frequency plasma [51] and microwave plasma assistance [52]. In the case of radio frequency CVD (RFCVD), the two-dimensional growth rate of graphene is 1000 times larger than thermal CVD at 750 °C [51]. Consequently, compared to thermal CVD, RFCVD can produce graphene with higher quality in similar temperature range. Guo et al. [66] reported in 2015 the use of molten Cu while utilizing methane as carbon precursor to synthesize high-quality monolayer graphene. Unfortunately, severe Cu evaporation in the reaction chamber happens simultaneously with the graphene growth stage. Recent study in 2016 by Sun et al. [40] showed the feasibility of directly form large-area high-quality graphene on solid glasses using methane with I_{2D}/I_G value from 1.6 to 2.5. Even if the defect level [67] of the as-produced graphene was quite high ($I_D/I_G > 1$), their work demonstrates the great potential of cheaper and scalable production route for graphene on insulating solid glasses.

After methane, acetylene is the most widely used gaseous carbon precursor to grow graphene via CVD. There have been many variations of studies performed to improve the process ecosystem and graphene quality. Yang et al. [68] investigated the effect of pre-oxidized pockets of Cu toward low-pressure CVD (LPCVD) graphene growth. The Cu foil is folded into pockets with the remaining three sides crimped with a pincer. Then, the pocket is pre-heated to form Cu_2O layer. At low acetylene flow rate, monolayer graphene with low defect density and large domain size was formed. Growth on metal oxides constitutes an important step toward graphene-based electronics [69]. Direct growth of graphene on non-interacting substrates would eliminate the transfer step and avoid the sacrifice of the used metal catalyst being the major roadblock for cheaper level of graphene synthesis [70]. In addition, Chen and Hsieh et al. [71] reported that the quality of few-layer graphene films could be increased by reducing the carbon concentration via reduction in acetylene flow rate at 600 °C in a LPCVD setup. The flow rate of acetylene is very vital as elevated acetylene flow rate may produce 'carbon smoke' that contaminates the CVD chamber. Monolayer graphene can also be grown on polycrystalline Cu foils isothermally in an ultra-high vacuum CVD (UHV-CVD) setup [72]. In 2013, Qi et al. [73] synthesized bilayer graphene films by atmospheric pressure CVD (APCVD) with acetylene on a Cu foil with different ratio of H_2 and Ar. It is suggested that H_2 acts as both soft etchant and activator for the bound carbon within the formed graphene. This shows that H_2 presence is also important for graphene growth using C_2H_2 as carbon precursor. Table 1 illustrates, in details, examples of graphene grown by CVD using various gaseous carbon precursors.

The use of gaseous carbon precursors is not just limited for graphene films synthesis, but other forms of graphene can also be produced. Trinsoutrot et al. [74] successfully synthesized 3D graphene networks on Ni foam between 750 and 850 °C at ambient pressure using ethylene as carbon precursor. The higher reactivity of ethylene as compared to methane allows the deposition temperature to be significantly reduced [75]. Addou et al. [76] have successfully grown monolayer graphene at ~ 550 °C using UHV-CVD from ethylene. At temperature below ~ 500 °C, competing carbide phase formation is reported to impede graphene formation. Meanwhile, Sagar et al. [77] grew graphene on Ni and Cu foils using ethylene as carbon precursor via CVD method. The pressure of the reaction was varied from 0.1 to 0.4 MPa to investigate the role of ethylene partial pressure on the growth of graphene layers with 0.2 MPa coming out on top for this particular setup. Besides that, propene (C_3H_6) has also been reported as a carbon precursor to grow graphene on Rh(111) by Gotterbarm et al. [78].

It is known that CVD using methane and hydrogen entails a high cost of instrumentation together with a high degree of safety precautions [79]. Both methane and hydrogen are extremely flammable and may form explosive mixtures with air. They are hazardous and asphyxiating gases since they can displace oxygen in an enclosed space; the same goes for ethylene and acetylene. However, there are advantages in using gas precursor. Firstly, gaseous precursor takes less space than liquid and solid precursor as they can be stored in specialized tank. Secondly, industries that produce gas precursors such as biogas as a by-product can be a direct supply line for graphene CVD. Biogas is primarily comprised of methane and

Table 1 Examples of graphene growth conditions using different gases as carbon precursor and their characteristics

Carbon precursor	Growth substrates	Growth conditions					Graphene morphology			References
		Method	Temperature (°C)	Pressure	Flow ratio	Reaction duration	Type	Raman	FWHM (cm^{-1})	
CH_4	Rhodium (111) foil Thickness = 25 μm	CVD	1000	1 atm	Ar:CH_4:H_2 = 200:12:50	10 min	Multilayer graphene	I_{2D}/I_G = 0.74	60	[64]
CH_4	Cu foil	CVD	1000	580 mTorr	CH_4:H_2 = 5:50	30 min	Monolayer graphene	I_{2D}/I_G = 2.3	32.8	[50]
CH_4	Quartz glass, borosilicate glass, sapphire glass	CVD	1020	1 atm	Ar:CH_4:H_2 = 100:8:50	3 h	Monolayer graphene	I_{2D}/I_G = > 2	32	[40]
CH_4	Cu foil Thickness = 6.3 μm Size = 16 × 16 mm	Radio frequency plasma CVD	750	5 Pa	CH_4:H_2 = 0.2:100	150 s	Monolayer graphene	I_{2D}/I_G = 2.4 I_D/I_G = 0.12		[51]
CH_4	Cu foil Thickness = 25 μm Size = 10 × 10 mm	Microwave plasma CVD	650	7 kPa	CH_4:H_2 = 5:500	40 s	Monolayer graphene	I_{2D}/I_G = 2.86	74.7	[52]
CH_4	Liquid Cu	Rapid CVD	1090	700 mbar	Ar:CH_4:H_2 = 960:40:5–30	5–10 min	Monolayer graphene	I_{2D}/I_G = > 2	30–40	[66]
C_2H_2	Cu foil Thickness = 25 μm	(UHV-CVD) vacuum cooling = 100 °C/min	900	5×10^{-7} mbar	C_2H_2:H_2 = 80:600		Monolayer graphene	I_{2D}/I_G = 1.9–2.6 I_D/I_G = 0.07–0.19		[72]
C_2H_2	Cu foil Thickness = 50 μm	CVD (fast cooling = 100 °C/min)	1035	0.8 torr	C_2H_2:H_2 = 2.8:80		Monolayer graphene	I_{2D}/I_G = > 2 I_D/I_G = 0–0.2	< 37	[68]
C_2H_2	Ni foil Thickness = 25 μm	Thermal CVD	600	133.3 Pa	C_2H_2:H_2 = 12:12		Few-layer graphene	I_{2D}/I_G = 0.4 I_D/I_G = 0.28		[71]
C_2H_2	Cu foil Thickness = 25 μm Area = ~ 6 cm^2	APCVD	1000	1 atm	C_2H_2:H_2:Ar = 1:100:900	10 min	Bilayer graphene	I_{2D}/I_G = 0.9–1.3 I_D/I_G = 0–0.1	44–59	[73]
Ethylene, C_2H_4	Ni foam Thickness = 1.8 mm Size = 40 × 60 mm	CVD	750–850	1 atm	C_2H_4 = 15	5–40 min	3D graphene 15 wt% of 3D graphene Thickness = 500–1000 nm			[74]
C_2H_4	Ni (111) single-crystal foil	CVD	550	10^{-6} Torr			Monolayer graphene			[76]
C_2H_4	Cu and Ni foil Thickness = 25 μm Area = ~ 1 cm^2	CVD	1050	0.2 MPa	C_2H_4:H_2:Ar = 40:40:160	7–10 min	Mono and few-layer graphene			[77]
C_2H_4	Cu film deposited on SiO_2/Si Cu thickness = 1 μm	Thermal CVD	860 °C	1 kPa	H_2:Ar = 100:1000		Bilayer graphene			[81]
C_3H_6	Rh(111) foil Thickness = 3 mm	CVD	700–1000 K	2×10^{-8} mbar			Graphene with low defect density			[78]

FWHM full width at half maximum

carbon dioxide which have been used before to synthesize graphene [80].

Gaseous carbon precursors are the main source of carbon feedstock for graphene production by CVD; liquid and solid precursors have already shown to have its own advantages. Next chapter will discuss the various liquid precursors that have been used as carbon source for graphene CVD recently.

Liquid carbon precursors

In the early years of graphene research, aliphatic linear hydrocarbon like methane has become the mainstay as it is easy to set up and very stable at elevated temperature. Once the theoretical groundwork was confirmed, the emergence of liquid and solid precursors becomes more apparent. It is expected to change the landscape of the graphene synthesis using CVD method, as liquid carbon precursors are easy to use and relatively inexpensive as compared to conventional gaseous one [82].

Srivastava et al. [83] involved the use of hexane (C_6H_{14}) with which large-area continuous and uniform graphene films were formed. This novel method has also allowed an easier way to dope graphene by using various organic solvents as liquid precursors containing dopant atoms. Since monolayer graphene has zero band gap, many researchers have identified the use of dopant to construct a band gap of its own. The use of organic solvents as liquid precursors containing the desired dopant atoms would allow a better process maneuverability in addition to a safer and cheaper synthesis route. Miyata et al. [84] managed to synthesize single-layer graphene from ethanol (C_2H_5OH) using flash cooling just after CVD. Detailed comparison of the flash cooling process against normal natural cooling suggests that the single-layer graphene growth occurs from surface diffusion of carbon atoms on Ni substrate and not from bulk carbon precipitation. Hence, liquid precursors also have similar dependency to that of gaseous precursors on the cooling step in order to produce monolayer or bilayer graphene. Kishi et al. [85] synthesized single-layer graphene on polycrystalline Ni foils by using isopropyl alcohol (C_3H_7OH) with an infrared lamp heating. However, the full width at half maximum (FWHM) of the graphene produced decreases in the Raman mapping using isopropyl alcohol, meaning that ethanol is better than isopropyl alcohol for synthesis of single-layer graphene.

Guermoune et al. [82] reported growth of monolayer graphene using methanol, ethanol and 1-propanol (C_3H_7OH) as liquid carbon precursor on Cu foil. The used precursor was transported through the reaction chamber using 3–5 freeze–pump–thaw cycles at 10^{-6} Torr. Interestingly, for these different chain length precursors Raman spectra of good quality were observed [86]. It also was found that the 2D band sharpened while the D band diminished indefinitely as the growth temperature was increased from 650 to 850 °C. The fitted Lorentzian changes from many layers to just one Lorentzian at 850 °C indicating a good quality monolayer graphene. These findings indicate that the number of bonds in the precursor is less significant than the growth temperature for graphene formation with alcohol.

Dong et al. [87] were able to synthesize large-area, continuous graphene films by APCVD using pentane (C_5H_{12}) or ethanol. The liquid precursors are conveyed through the reaction chamber by using H_2/Ar gas mixture. It was found that graphene grown from ethanol has higher Hall mobility, lower sheet resistance and lower defect density than the one grown from pentane. Besides ethanol, benzene (C_6H_6) is one of the most popular and effective liquid precursor for graphene synthesis. Li et al. [56] used benzene as liquid hydrocarbon source and obtained monolayer graphene flakes at a very low reaction temperature of 300 °C. Benzene molecules were suggested to only need dehydrogenation before it can interconnect with each other on top of the metal substrate Cu to form graphene. However, no graphene was found due to insufficient energy at 200 °C, probably temperature is too low to remove hydrogen and form any graphene. This finding implies that benzene basic structure has an instrumental impact toward the process of graphene synthesis.

John et al. [88] used ethanol to produce graphene on commercially available stainless steel by using APCVD. Mono-, bi- and tri-layer graphene were formed over a large area verified by optical microscopy and Raman spectroscopy. However, there were a number of oxide species adsorbed on the grown graphene. Choi et al. [89] used benzene as carbon source to produce monolayer graphene at a very low growth temperature of 300 °C. By using density functional theory (DFT) and transition state theory (TST) calculations together, the dehydrogenation times (t_D) were calculated. At 300 °C, the t_D for graphene growth using benzene was estimated to be

around 6.5 s while at 200 °C, it was around 20 min. The long t_D rules out the prospect of graphene synthesis at such a low temperature since the molecules must adsorb on the metal catalyst to create carbon–carbon bonds with other dehydrogenated precursor molecules or carbon active species.

A recent publication by Seo et al. [90] has been touted to be the solution for low-cost synthesis of graphene. Here, soybean oil was used as the carbon source for graphene synthesis while the main emphasis was on exploiting the ambient air as the filler for the CVD. Normally, highly purified compressed gases such as N_2, Ar and H_2 were used to create a highly controlled environment for graphene growth. However, single to few layers of continuous graphene films were converted from a renewable natural precursor in the form of soybean oil. The CVD technique is significant since it opens a new avenue to other types of renewable precursors that may also have the potential to be used similar to soybean oil. Other than soybean oil, there have been several other complex carbon precursors reported in the field of graphene synthesis such as waste chicken fat [59], commercial palm oil [91] and refined cooking palm oil [92]. Among them, waste chicken is very promising as it represents a huge portion of the waste from the poultry processing industries. The technology to convert waste materials to high-quality product is always a good way to maximize a process earning potential with existing resources.

Han et al. [93] use also benzene to grow graphene on Cu(111) face in an ultra-high vacuum chamber via CVD. Benzene carbon precursor was purified by cycles of a freeze–pump–thaw method and then dosed into the chamber via a leak valve. XPS characterization showed that the C–C sp^2 bonding is predominantly preserved with an energy gap of 0.8 eV. In order to modulate electrical properties of graphene, the ability to dope graphene is critical. Conventional CVD method using melamine or ammonia at high growth temperature produced N-doped graphene with high defect density, low carrier mobility and low doping level. On the other hand, Xue et al. [94] demonstrated the synthesis of highly N-doped graphene at temperature as low as 300 °C by using pyridine (C_5H_5N) as carbon precursor. The doping process depends on formation of carbon–nitrogen bonds competing with carbon–carbon bond creation. High-temperature region was found to suppress the doping of nitrogen to favor C=C bond formation [95]. The use of pyridine as carbon precursor allowed the synthesis of graphene at low temperature [94]. Like for benzene, dehydrogenation pathway of pyridine easily provides active species being then able to deposit onto the metal substrate chosen. Effective dehydrogenation temperature for pyridine is indeed lower than that of its hexahydric ring decomposition temperature (620–650 °C) [96]. If a temperature above 650 °C is used, the hexahydric ring decomposes and supplementary energy will be needed for C and N atom active species to combine again which is a redundant and a wasteful endeavor. Lastly, a recent study by Jang et al. [49] has shown synthesis of high-quality monolayer graphene with optical transmittance of 97.6 and 100% surface coverage at 300 °C from benzene. A new step was introduced in their method; it consists of cycles of pumping and purging the reaction chamber before the CVD growth stage. This additional step avoids presence of oxidizing impurities during the graphene growth process and yields an oxygen-free APCVD process. Graphene film could also be formed at temperature as low as 100 °C with this process. However, the as-grown graphene contains here reduced surface coverage [49]. As a summary, Table 2 represents the details of graphene CVD using various liquid carbon precursors along with the morphology of the graphene produced.

The use of liquid precursor is opening a new frontier in the field of graphene synthesis. By simple observation, although the most commonly used liquid carbon source for graphene growth is ethanol, the super-effectiveness of benzene has made it much more popular in recent times. It certainly raises some very interesting questions regarding the feasibility of liquid benzene as a solution for low-cost graphene production and the mechanism behind its unique properties compared to other carbon sources. Liquids require a means to convert the liquid precursor into gaseous form before it reaches the active metal catalyst region as opposed to gas precursors. Some of the liquid precursors are volatile organic compounds (VOC) and carcinogenic in nature making it quite harmful to human health. Hence, high-end safeguard system is also compulsory to safeguard the well-being of the operators. Liquid precursors such as benzene and pyridine can synthesize graphene at around 300 °C without the need of plasma-enhanced CVD. Reduction in the graphene growth reaction temperature directly lessens the cycle time of graphene CVD

Table 2 Examples of graphene growth by CVD using liquid carbon precursors

Carbon precursor	Growth substrates	Growth conditions					Graphene morphology			References
		Method	Temperature (°C)	Pressure	Flow ratio	Reaction duration (min)	Type	Raman	FWHM (cm^{-1})	
Ethanol, C_2H_5OH	Ni Thickness = 25 μm Size = 3 × 3 cm	CVD	850	1 Torr	H_2 = 10	5	Monolayer graphene	I_{2D}/I_G = > 2		[84]
Ethanol	Stainless steel, SS304 Thickness = 0.1 mm Size = 1 × 1 cm	Direct thermal CVD	850	1 atm		10	Mono-, bi-, tri-layer graphene			[88]
Ethanol	Ni foil Thickness = 10 μm Size = 1 × 1 cm	IR heating system	1000	1 atm		5	Monolayer graphene	I_{2D}/I_G = 3.5	30–35	[85]
Hexane, C_6H_{14}	Cu Thickness = 25 μm Size = 3.5 × 1.5 cm	CVD	950	500 mTorr		4	Monolayer graphene		40 ± 4	[83]
Pyridine, C_5H_5N	Cu	CVD	300	1 atm			Monolayer N-doped graphene	I_D/I_G = 0.16 I_{2D}/I_G = 4.7		[94]
Methanol, CH_3OH Ethanol, 1-propanol, C_2H_5OH	Cu Thickness = 25 μm	CVD	850	1 Torr	H_2 = 10	5 min	Monolayer graphene	I_{2D}/I_G = ~ 2–3		[82]
Pentane, C_5H_{12} Ethanol	Cu Thickness = 50 μm	APCVD	900	1 atm	Ar:H_2 = 1000:10	30 min	Mono-, bi-, few-layer graphene			[87]
Benzene, C_6H_6	Cu foil	CVD	300	8–15 Torr	H_2 = 50	15–30 min	Monolayer graphene flakes	I_{2D}/I_G = 2	38	[89]

Table 2 continued

Carbon precursor	Growth substrates	Growth conditions					Graphene morphology			References
		Method	Temperature (°C)	Pressure	Flow ratio	Reaction duration (min)	Type	Raman	FWHM (cm^{-1})	
Benzene	Cu Thickness = 25 μm	Oxygen-free APCVD	300	1 atm	Ar:H_2 = 5:20	5 min	Monolayer graphene	I_{2D}/I_G = > 1.8		[49]
Benzene	Cu Thickness = 10 μm	CVD	300	8–15 Torr	H_2 = 50	15 and 30 min	Monolayer graphene flakes		38	[56]
Benzene	Cu (111) Size = 12 × 5 mm^2	CVD	437	1 × 10^{-10} mbar		50 min	Multilayer graphene			[93]
Soybean oil	Ni Thickness = 25 μm	APCVD	800 (30 °C/min)	1 atm		3 min	Monolayer graphene	I_{2D}/I_G = 0.95–1.50 I_D/I_G = 0.15–0.25		[90]
Cyclohexane, C_6H_{12}	Cu_2NiZn ternary alloy	LPCVD	1000	300–600 mTorr		3–20 min	Monolayer graphene	I_{2D}/I_G = ~ 4.8		[97]
Commercial palm oil	Ni Thickness = 100 μm Size = 1 cm^2	APCVD	1100	1 atm			Multilayer graphene	I_{2D}/I_G = 1.54 I_D/I_G = 0.73	> 50	[91]
Refined cooking palm oil	Thickness = 100 μm	CVD	900		Ar:H_2 = 50:200	15 s	Mono-, bilayer graphene	I_G/I_{2D} = 0.62	27	[92]
Waste chicken fat	Cu Thickness = 20 μm	LPCVD	1080	150 Pa	Ar:H_2 = 98:2	60 min	Monolayer graphene	I_{2D}/I_G = > 3 I_D/I_G = < 0.1	~ 34	[59]

FWHM full width at half maximum

and the overall energy that is required to reach the standard reaction temperature for methane which is around 1000 °C, especially if it is a hot-wall CVD. Of course, benzene and pyridine also come with their own baggage in that they are human carcinogens. As long as the drawbacks can be managed, liquid precursors seem to have a bright future in low-cost large-scale production of high-quality graphene.

Solid carbon precursors

There are many research works dealing with the use of a solid carbon precursor in graphene synthesis by CVD. They can be complex in terms of their chemical and biological structure, especially those that are parts of a living creature [98, 99]. Ruan et al. [98] grew high-quality graphene from a number of raw carbon precursors at 1050 °C under vacuum environment. The used carbon precursors include grass, plastic, dog feces, cockroach leg, cookie and chocolate, which represent foods, wastes and insect-derived carbon sources. For the CVD growth, the solid carbon precursor was placed on top of the Cu foil while pristine monolayer graphene formed on the backside of the Cu substrate by CVD [98]. The formation of high-quality graphene at the bottom of the side of the Cu foil comes as a surprise considering that Cu has low solubility of carbon even at high temperature at 1050 °C (0.001–0.008 wt% solubility at ~ 1084 °C for Cu) [100, 101]. Moreover, the reaction chamber was under high vacuum conditions with Ar and H_2 flow of almost 600 sccm. In theory, the carbon precursor should have evaporated away before reaching the effective carbon deposition temperature.

Meanwhile, Sun et al. [102] have demonstrated the synthesis of N-doped and pristine monolayer graphene by using PMMA as a solid carbon source at 800 °C with melamine ($C_3N_6H_6$) as source for nitrogen. The N-doped graphene was obtained by mixing melamine, a doping reagent with PMMA, and spin-coated onto the Cu surface. Aside from that, fluorene ($C_{13}H_{10}$) and sucrose ($C_{12}H_{22}O_{11}$) were also used. Interestingly, both solid carbon precursors were able to produce high-quality graphene even though these precursors contain probable topological defect initiators. Sucrose contains high concentration of heteroatoms oxygen while fluorine includes a five-membered ring differing from the typical six-membered aromatic ring of graphene. It was suggested that the dissociated C obtained at elevated temperature has a higher affinity for the transition metal Cu catalyst surface than O heteroatoms. Plus, most of the topological defects are self-healed as the graphene was formed. Choi et al. [89] was also another success story when monolayer graphene was synthesized at 300 °C with *p*-terphenyl as carbon precursor. First-principle-based multi-scale modeling was performed and showed that the growth temperature can be reduced significantly from 1000 to 300 °C as methane is replaced by *p*-terphenyl which is in agreement with the experimental tests. It was suggested that the London dispersion force is the source of the growth temperature reduction. In fact, the London dispersion forces enhance the adsorption energies, which prevents desorption, facilitates dehydrogenation and promotes graphene growth at a lower temperature.

Ray et al. [99] reported a simple general method for preparing nickel-decorated graphene nano-powder by using hibiscus and lotus flower petals via thermal exfoliation. The presence of nickel seems to enhance the graphene electron density near the Fermi energy level. More significantly, by using flower petals as the carbon feedstocks, the use of hazardous chemicals can be avoided while maximizing the importance of cheap natural resources for a brighter future for economical and eco-friendly large-scale synthesis of graphene. However, the best results were attained at very high temperature of 1600 °C. This is due to the high energy level needed to facilitate the removal of oxygen-containing molecules. The use of high temperature for graphene synthesis negates the impact of cheaper natural carbon sources on the synthesis cost. This was down to how the metal substrate was planted into the reaction [99] which is via wet chemical soaking. Table 3 shows a comprehensive list of various solid carbon precursors used to produce graphene via CVD along with the graphene growth conditions and the synthesized graphene quality.

Asphalt is another candidate of carbon precursor. Produced as a by-product from petroleum distillation, it has not been widely used in the downstream process due to its very complicated structure and unworkability. Interestingly, asphalt contains a large amount of carbon-rich compounds with alkyl chains linked to aromatic cores [103]. Liu et al. [104] used CVD to convert the disordered asphalt into ordered multilayer 3D graphene. In addition to asphalt, waste plastics have also been proven to be able to synthesize high-quality single-crystal graphene [105]. Gas

Table 3 Examples of graphene grown by CVD using solid carbon precursors

Carbon precursor	Growth substrates	Growth conditions					Graphene morphology			References
		Method	Temperature (°C)	Pressure	Flow Ratio	Reaction duration (min)	Type	Raman	FWHM (cm^{-1})	
PMMA ($C_5H_2O_8)_n$, polystyrene	Cu foil Thickness = 25 μm	CVD	800	8–15 Torr	H_2 = 50	45	Monolayer graphene	I_G/I_{2D} = 0.5	37	[56]
PMMA, sucrose ($C_{12}H_{22}O_{11}$), fluorine ($C_{13}H_{10}$)	Cu foil Size = 1 × 1 cm	LPCVD	800	Low	Ar:H_2 = 500:50	10	Pristine and n-doped graphene	I_{2D}/I_G = 4 I_D/I_G = < 0.1	30	[102]
PMMA, high-impact polystyrene (HIPS), acrylonitrile–butadiene–styrene (ABS)	Cu foil Thickness = 25 μm	APCVD	1000	1 atm	CH_4:H_2 = 20–100:50–600		Bilayer graphene	I_{2D}/I_G = > 1.3 I_D/I_G = ~ 0.7	60	[106]
p-terphenyl ($C_{18}H_{14}$)	Cu foil	LPCVD	300	8–15 Torr	H_2 = 50	45	Monolayer graphene	I_{2D}/I_G = ~ 2	~ 35	[89]
Hexachlorobenzene, C_6Cl_6	Cu	Modified CVD	360	1 atm	Ar:H_2 = 400:100	5 min	Multilayer graphene flakes			[123]
Coronene, $C_{42}H_{18}$	Ru (0001)	Thermal CVD	827	Ultra-high vacuum			Graphene nano-clusters (GNCs)			[130]
Hexabenzocoronene $C_{48}H_{24}$	Co (0001)	Thermal CVD	327	3×10^{-11} Torr		20 min	Monolayer graphene			[128]
Cookie, chocolate, grass, dog feces, polystyrene, cockroach leg	Cu foil	LPCVD	1050	9.3 Torr	Ar:H_2 = 500:100	15	Monolayer graphene			[98]
Lotus, hibiscus flower petals	Ni nanoparticle	CVD	1600	Vacuum		30	Multi- and monolayer nickel-decorated graphene nanoparticle			[99]
Asphalt	Ni foam	CVD	940	1500 Pa	Ar:H_2 = 300:30	10	Multilayer 3D graphene	I_{2D}/I_G = 0.37		[104]
Amorphous carbon	Cu foil Thickness = 25 μm Size = 1 × 5 cm	CVD	1035	20 mTorr	H_2 = 2	30	Monolayer graphene	I_{2D}/I_G = 3	28	[120]
Amorphous carbon	Ni sputtered onto SiO_2/Si substrate	Filtered vacuum CVD	1000	Vacuum		5	Few-layer graphene			[119]
Highly oriented pyrolytic graphite (HOPG)	Ni deposited on HOPG Thickness = 100 nm Size = 2 × 2 cm	CVD	650	~ 5×10^{-8} Torr		1080	Monolayer graphene	I_{2D}/I_G = 3.23		[131]
Functionalized CNTs	Cu foil	CVD	1080	7 Torr	Ar:H_2 = 500:50	15	Rebar graphene	I_D/I_G = < 0.1		[122]
Phenyl-C_{61}-butyric acid methyl ester (Fullerene derivative)	Ni foil	CVD	800	1 Torr		5	Multilayer graphene			[121]
Waste plastic	Cu foil	APCVD	1020	1 atm	Ar:H_2 = 98:2.5	10	Monolayer graphene			[105]
Camphor ($C_{10}H_{16}O$)	Cu foil	APCVD	1020	1 atm			Monolayer and bilayer graphene			[113]
Camphor	Ni foil Size = 5 × 5 mm	APCVD	870	1 atm		2	Single-layer to few-layer graphene	I_{2D}/I_G = 9	21	[112]
Camphor	Ni foil Size = 2 × 2 cm^2	APCVD	700–850	1 atm			Few-layer graphene			[61]
Thiocamphor ($C_{10}H_{16}S$)	Cu foil Thickness = 0.025 mm Size = 5 × 5 mm^2	APCVD	1000	1 atm	Ar:H_2 = 485:15	15	Few-layer thiolated graphene	I_{2D}/I_G = 0.5	70	[60]

FWHM full width at half maximum

chromatography–mass spectrometry (GC–MS) showed that the waste plastic used was primarily comprised of polystyrene $(C_8H_8)_n$ and polyethylene $(C_2H_4)_n$. The polymer-based plastic is generally used in packaging industries. The effective use of waste plastic as carbon precursor for graphene synthesis can have unbelievable impact toward waste management and recycling process.

Graphene cannot be formed if the reaction temperature is lower than 600 °C by CVD using methane as carbon precursor, whereas CVD using solid PMMA and polystyrene was reported to be able to synthesize monolayer graphene at even 400 °C. Therefore, in retrospect, some of the CVD growth routes using solid carbon sources are more efficient than CVD using gaseous precursors at low temperature [56]. In 2011, Peng et al. [106] reported a transfer-free method to produce bilayer graphene directly on SiO_2 substrate using polymer films such as high-impact polystyrene (HIPS) and acrylonitrile–butadiene–styrene (ABS) as carbon source. The growth of graphene was achieved by carbon diffusion through the Ni layer through a bulk-mediated growth mechanism [107]. Figure 2 illustrates the process flow of the transfer-free bilayer graphene growth. While the method eliminates the need of any graphene transfer process, the technique still requires an etching stage to remove the thermally deposited Ni layer to expose the bilayer graphene deposited on top of SiO_2.

Solid botanical derivative camphor has also been used as carbon precursor to produce graphene. In fact, natural precursors were widely used to produce CNTs before the rise of graphene as the superior material became apparent to the scientific community [108–111]. Somani et al. [61] are one of the earliest researchers to investigate the feasibility of using for graphene synthesis by CVD. Ahmed et al. [112] successfully produced monolayer graphene from camphor using similar setup with a temperature of 870 °C. Aside from Ni, Cu has also been utilized as the metal substrate for graphene synthesis using camphor [113]. As Ni was used, 850 °C was sufficient to catalyze monolayer graphene formation. The utilization of Cu was observed to require higher temperature (1020 °C) so that monolayer graphene can be synthesized. In addition to that, thiocamphor which is another form of camphor has also been used to produce thiolated few-layer graphene [60]. Thiolated graphene has emerged as a suitable platform for anchoring semiconductor quantum dots for novel hybrid nanostructures [114]. There have been several reports in thiolated graphene synthesis via chemical reaction of reduced graphene oxide with propylene sulfide [115] and diazonium salt of 4-aminothiophenol [116]. Using thiocamphor in a CVD process as carbon precursor for both carbon and sulfur for the thiolated graphene can simplify the doping process altogether. This technique avoids the need of a two-step process for the conventional CVD-doping method by combining them into one process, reducing the thiolated graphene synthesis cycle considerably.

At the moment, graphite has been used extensively to produce graphene using the top-down method where graphite is exfoliated into thin graphene flakes by using the wet chemical exfoliation method [117, 118]. Graphite is available abundantly and is very cheap. Other forms of carbon allotrope have been used as carbon precursor via the CVD route in recent time. The applicability of amorphous carbon as carbon precursor for graphene growth can open up a new range of possibilities in graphene research and development. Seo et al. [119] presented the feasibility of using amorphous carbon to synthesize few-layer graphene. However, the method requires a two-step deposition process (Ni film deposition and a-C coatings) and from the study done only low quality of few-layer graphene was synthesized. In another work, amorphous carbon was deposited by an RF sputter on Cu foil [120]. From the study, it was established that monolayer graphene was formed only in the presence of H_2 that suggests the importance of H_2 in graphene growth process. Unfortunately, the process was performed under vacuum condition (20 mTorr) which is not favorable for the overall cost of the process.

It was also possible to form graphene using CVD from fullerenes, by using, for example, phenyl-C_{61}-butyric acid methyl ester (PCBM), a fullerene derivative [121]. In contrast to CNTs, the as-produced graphene does not exhibit the unique characteristic of rebar (reinforced bar) graphene [122]. For the graphene synthesis, a solution of PCBM in chlorobenzene was spin-coated on a nickel layer PCBM. Figure 3 shows the schematic illustration of the used process. A modified CVD method using hexachlorobenzene (HCB) at 360 °C was performed by Gan et al. [123].

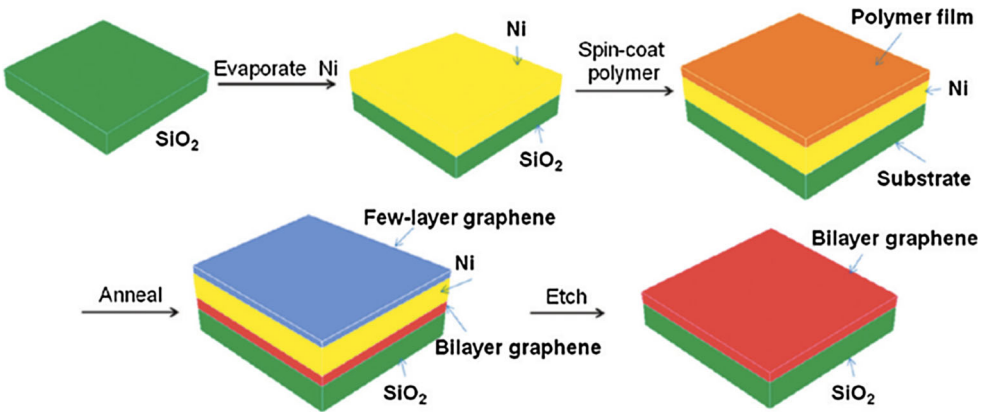

Figure 2 Schematics of bilayer graphene growth using spin-coated polymer films via carbon diffusion through Ni layer. Reprinted with permission from [106].

HCB is an aromatic organochloride with the molecular formula C_6Cl_6. Instead of dehydrogenation, HCB requires dechlorination before it can coalesce to form graphene. Interestingly, XPS analysis proved that $CuCl_2$ molecules were produced because of the redox reaction between Cu and HCB. The idea of converting a persistent organic pollutant, which has serious adverse effects to the human health and the environment to high-value product such as graphene, is certainly an attractive outlay [124, 125]. Wong et al. [126] used a much more complex coronene-based carbon precursor in the name of hexabenzocoronene (HBC) in graphene CVD process. The molecular structure of HBC consists of a central coronene molecule surrounded by six aromatic benzene rings. They exist in the form of solid at room temperature and can be used for photovoltaic [126] and super-capacitor applications [127]. Eom et al. [128] managed to grow epitaxial graphene monolayers on Co(0001) surface by using HBC at 327 °C. Furthermore, another fascinating carbon precursor that has been used for graphene CVD is coronene ($C_{24}H_{12}$). Coronene molecular structure can be described as a typical nanographene configuration except that hydrogen atoms saturate its edges [129]. The form of graphene synthesized from coronene is highly dependent on the reaction temperature during the CVD reaction. At 627 °C, graphene nano-clusters (GNCs) with the similar seven C_6-ring structures as coronene were present but without the peripheral hydrogen atoms at its edges, while only monolayer graphene structures were observed at 827 °C.

As a summary, even complex biological materials such as flower petals [99], cookies and chocolate [98] were demonstrated to be suitable candidates as precursors for graphene synthesis. Stronger and better form of graphene called rebar graphene was also produced by using carbon nanotube as carbon source [122]. However, most of the studies involve the use of high temperature reaction condition which is not a good sign for the development of large-scale graphene production. From the previous discussion, it is clear that solid carbon sources can play a vital role in CVD synthesis of high-quality graphene. The variation of solid carbon precursors used signifies the robustness of the CVD process for graphene growth.

As a whole, solid precursors are comparable to liquid precursor in that it requires an external source of energy to convert it into gaseous phase before it makes contact with the metal catalyst. Hence, comprehensive and costly extra setup is required. Additionally, solid precursors will definitely take a lot

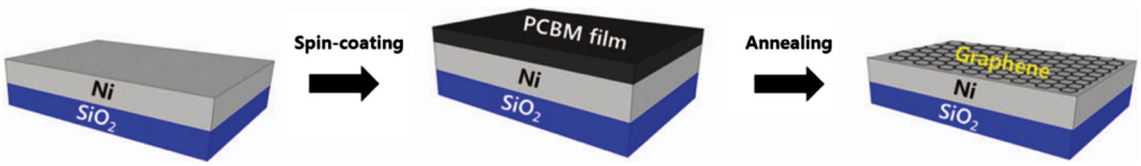

Figure 3 Schematic illustration of graphene synthesis with PCBM as carbon precursor. Reprinted with permission from [121].

more spaces than either gas or liquid precursors. However, most of the solid precursors used are unutilized wastes and have negative economic value to the society. Converting these wastes into high-value products in the form of graphene while also reducing the cost of graphene synthesis is a big positive of using solid precursor as raw material for graphene. Some of the solid precursors such as *p*-terphenyl, hexachlorobenzene and hexabenzocoronene also exhibit similar feature to benzene and pyridine in having low reaction temperature for graphene growth even though they have different physical states at ambient room temperature. This phenomenon gave some clues in which what were the pivotal factors in this unusual lower energy requirement for graphene growth and will be discussed in a more detailed manner in the next chapter.

Mechanisms of carbon precursors in graphene CVD

Carbon precursor is a key parameter in graphene synthesis, especially as the temperature used is very low since the catalytic power of the metal used for the synthesis will not be optimized. From the previous discussion regarding the various types and nature of the reported carbon precursors, the mechanism involving in the graphene formation seems not to be only directly correlated with the physical state of the used carbon precursor. Carbon precursors containing simple aliphatic linear hydrocarbon chains [74, 132] react differently from those made of aromatic compounds [93, 94]. Similar pattern was observed for aromatic compounds such as benzene [49], pyridine [94], hexachlorobenzene [123], hexabenzocoronene [126] and *p*-terphenyl [89] which require lower reaction temperature for graphene growth (300–450 °C) than methane (~ 1000 °C) which is an essentially aliphatic compound. What is the fundamental reason for this phenomenon? Instead of the precursor physical state, the chemical structure of the compound itself appears to be a more relevant parameter. Based on the extensive exploration of previous studies, the mechanisms involved in graphene synthesis by CVD can be mainly divided into three important characteristics of the carbon precursors: (1) aliphatic compounds; (2) aromatic compounds; (3) CNT unzipping. Each of them will be discussed in the following sections.

Aliphatic compound precursors

Methane, acetylene and ethylene have been extensively studied in the past, and the mechanisms involved in graphene CVD growth for these carbon precursors are fairly established compared to other precursors. As a carbon source, the required output is to transform it into active carbon species. At high temperature, the metal substrate becomes active and the energy barrier for precursor dissociation is lowered to a feasible level [133]. For methane, it only needs to be dehydrogenated before it can be used as a building block for graphene growth [107]. For acetylene and ethylene, there is another reaction after dehydrogenation to break the carbon–carbon bonds. However, these carbon–carbon intermediates are highly difficult to dissociate. During dehydrogenation of methane on Cu surface, all four dehydrogenation steps are endothermic and there are three intermediates formed, namely methylidyne [CH_3], methylene [CH_2] and methyl [CH] radicals as shown in Fig. 4. Similarly, intermediate compounds are as well formed as acetylene and ethylene are used as carbon precursor. Some polymer such as polystyrene also exhibits a similar mechanism by considering it as a macromolecule with repeated subunits of C_8H_8 [56, 106].

Among them, acetylene has the highest dehydrogenation energy with 506 kJ/mol, followed by ethylene with 443 kJ/mol and lastly methane with 410 kJ/mol [135]. The easier dissociation and dehydrogenation of methane allows to better control the graphene layer quantity and growth rate [133, 136]. Besides that, methane adsorption energy is relatively low which reduces the carbon active species supply to the CVD reaction [134]. The induced decrease in carbon active species can lead to low growth rate for graphene, and that results in long growth duration and consumption of large amount of carbon precursors and energy. If the growth duration becomes irrational to the cost of production, hydrocarbon gas precursors with high reactivity and surface adsorption energy such as acetylene that can reduce the graphene growth time should be considered [72]. Methane is the most widely used carbon precursor for graphene CVD because of its low pyrolysis rate. Acetylene and ethylene on the other hand provide a higher pyrolysis rate that can increase the defect density of the grown graphene due to the divacancy defect healing mechanism [137]. However, it can be

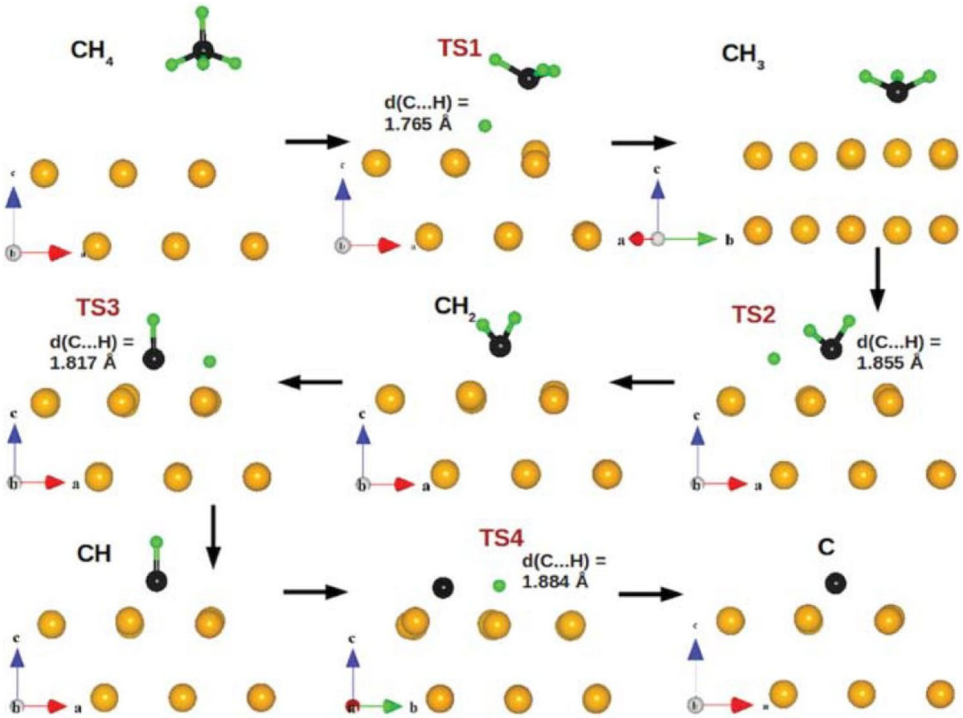

Figure 4 Diagram of methane dehydrogenation from the side view. Orange sphere = transition metal atom; green sphere = hydrogen atom; black sphere = carbon atom; ts = transition state. Adapted with permission from [134].

used for low-temperature graphene synthesis by CVD because of its low pyrolysis temperature (450 °C) [137]. While acetylene and ethylene can produce graphene at a lower reaction temperature, methane provides better stability and robustness in terms of graphene layer control and homogeneity of its growth: properties that make graphene the standout material of the last decade.

Non-hydrocarbon compounds include compounds such as ethanol [82, 88] and methanol [82] that contain other elements aside from carbon and hydrogen including oxygen, nitrogen or sulfur. Non-hydrocarbon precursors follow a growth mechanism comparable to that of hydrocarbons; added to dehydrogenation, denitrogenation and deoxygenation also occur. In the final stage of the process, intermediates and carbon active species react with each other if the proper conditions are used and form graphene on top of the metal substrate. Although the raw carbon precursor might contain other chemical elements such as oxygen, nitrogen and sulfur, most of them will pass through the reaction chamber without reacting with the transition metal catalyst. This phenomenon was confirmed by using XPS to verify the chemical environment and the elemental composition of the graphene when cookies, grass and chocolate were used as carbon precursors [98]. No other elements were found in the XPS confirming the graphene high purity even though the carbon source consists of a mixture of complex compounds. However, if the right conditions are met, some of these elements will react with graphene. Such incidence was found when thiocamphor was used as carbon precursor [60]. As a result, thiolated few-layer graphene was synthesized with the sulfur coming from the thiocamphor itself.

Aromatic compound precursors

Compared to other carbon precursors, aromatic compounds represent the most interesting opportunity and potential to the field of graphene grown by CVD. Benzene [49], pyridine [94], hexachlorobenzene [123], hexabenzocoronene [126] and *p*-terphenyl [89] are aromatic compounds that have been studied and showed a different pathway to graphene growth. As already mentioned, lower growth temperatures can be used when aromatic compounds are chosen as the carbon precursor for graphene formation (~ 300 °C). The low level of energy required for graphene

growth from C_6H_6 has been attributed to its basic structure analogous to the hexagonal honeycomb structure of graphene. However, the dehydrogenation time (t_D) of C_6H_6 was calculated to be in a reasonable range even at temperature as low as 300 °C as observed from Table 4. Conversely, the t_D for CH_4 was estimated to be around 440000 s at 300 °C that is not compatible with a CVD process. It is intriguing that graphene can be produced at 300 °C by using benzene, considering the metal substrate is not active at this low temperature level. In this particular case, carbon precursor is incontestably a primary relevant factor for graphene growth.

Low t_D is highly desirable to favor graphene formation since hydrogen atoms are easily removed and it takes then shorter time to form carbon active species which are the building blocks for graphene growth. As temperature reduces, the t_D became too long and graphene growth is no longer feasible. Hydrogen-containing molecules do not have sufficient time to remove hydrogen atoms and formation of graphene is compromised. This is the case for *p*-terphenyl ($C_{18}H_{14}$) at 200 °C [89], while continuous monolayer graphene was obtained at 300 °C using *p*-terphenyl with a symmetric 2D peak at around 2685 cm^{-1} that can be well fitted with a FWHM of approximately 35 cm^{-1} [138, 139]. The t_D at 200 °C was simply too long (3300 s) for graphene growth to make any sense. Even with a t_D of 43 s at 600 °C, graphene formation was not achieved when methane was used as the carbon precursor.

For HCB, in the same way dechlorination reaction has to take place before graphene formation. Figure 5 illustrates a simple schematic diagram for CVD of graphene from HCB. The presence of Cu in the reaction can efficiently enhance dechlorination phenomenon during the process. The drastically decrease in the reaction temperature to 300 °C [123, 124] was attributed to its basic structure forming a C_6 ring after dechlorination.

Pyridine is another form of aromatic ring with nitrogen and carbon within its heterocyclic ring. Dehydrogenation of pyridine can also be done at quite low temperature, around 300 °C [94]. Direct synthesis of monolayer nitrogen-doped graphene can take place even though high defect density is normally reported [140]. However, formation of nitrogen-doped tetragonal-shaped single-crystal graphene (NTSG) arrays with I_D/I_G ratio around 0.16, lower than typical value for polycrystalline N-doped graphene, was also reported (Fig. 6) [94].

Choi et al. [89] found that the London dispersion forces enhanced the adsorption energies of aromatic molecules by about 0.5–1.8 eV. Consequently, the active species involved will have a longer adsorption period for the dehydrogenation process and graphene growth can be performed at considerably lower temperatures. London dispersion is a key element of the more popularly recognized van der Waals forces. London dispersion forces are weak interactions among multipoles and transient dipoles related to various parts of matter [141]. As discussed earlier, from aromatic benzene reactive hexahydric ring active species are incorporated onto the graphene nuclei edges that are chemically active to continue the graphene growth. Previous methods of using benzene as carbon precursor only resulted in the yield of graphene flakes with a size limited to several micrometers [56, 89]. Plus, low-pressure CVD leads to reduce catalytic dehydrogenation and C–C bond formation resulting in limited areas of graphene [89, 93, 142]. At ambient pressure, graphene nucleation can occur at a sufficient rate. However, the presence of oxygen species in the reaction chamber

Table 4 Estimated dehydrogenation time, t_D for CH_4, C_6H_6 and $C_{18}H_{14}$ at different temperatures. Reprinted with permission from [89]

Temperature	Estimated t_D (in s)		
	CH_4	C_6H_6	$C_{18}H_{14}$
1000 °C	0.18	8.4×10^{-4}	5.2×10^{-8}
800 °C	1.6 (✔)	3.2×10^{-3}	8.5×10^{-7}
600 °C	43 (✗)	2.3×10^{-2}	4.9×10^{-5}
400 °C	8.1×10^{3}	0.57	2.9×10^{-2}
300 °C	4.4×10^{5}	6.5 (✔)	3.6 (✔)
200 °C	1.4×10^{8}	1.2×10^{3} (✗)	3.3×10^{3} (✗)

(✔ = graphene growth achieved; ✗ = graphene growth not achieved)

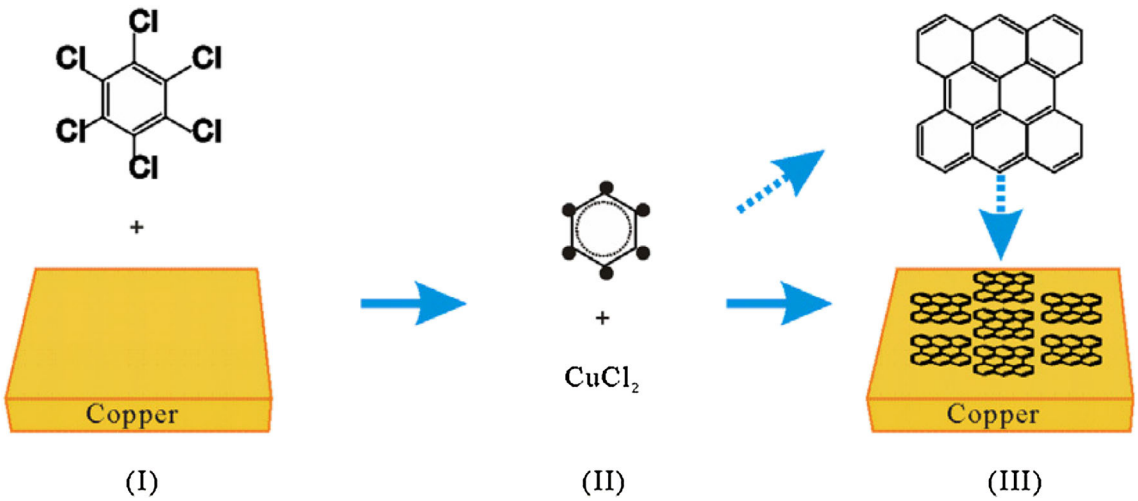

Figure 5 Schematic of graphene flake CVD growth by using hexachlorobenzene. Reprinted with permission from [123]. Stage I: Cu and HCB react and prompt the dechlorination of HCB; Stage II: HCB molecules entirely dechlorinate to form the media product C_6 rings and $CuCl_2$; Stage III: The produced media C_6 rings assembled together and form graphene on Cu surface.

during graphene growth can yield a defective carbon film with amorphous carbon regions. Residual oxygen is known to etch the as-grown graphene [95]. Son et al. [143] used mild oxidant in the form of carbon dioxide resulting in the formation of a thin layer of nickel oxide on the Ni surface. The formation of this sub-oxide layer suppresses the diffusion of C active species into the bulk Ni, suggesting that a surface-growth mechanism instead of the conventional bulk-mediated mechanism in Ni [34]. Contrary to previous study, Strudwick et al. [80] used the mild oxidation ability of carbon dioxide to remove preexisting and emerging carbon impurities and etch carbon of lesser quality from being deposited during graphene growth. However, mild oxidant can lead to damage the as-grown graphene. In that case, oxygen-free APCVD would become the ideal scheme as shown in Fig. 7. The aromaticity of the carbon precursor appears to be very crucial in obtaining the low temperature for graphene growth CVD. Cyclohexane, for example, is a cyclic compound that has comparable makeup to graphene. However, it may undergo pyrolysis similar to hexane, an aliphatic compound than benzene. This phenomenon can be observed from the work of Gan et al. [97] who reported the synthesis of monolayer graphene from cyclohexane at 1000 °C via ternary Cu_2NiZn alloy metal catalyst.

Another interesting aromatic compound that has been used to produce graphene is asphalt [104]. Asphalt is not a pure aromatic compound. Asphalt is far more complex than the other aromatic compounds that have been discussed. Unlike the other aromatic compounds, asphalt contains small planar aromatic structures with some additional functional groups compounds such as sulfur, alkyl and nitrogen [144]. Instead of using asphalt directly inside of the reactor chamber, the Ni foam was coated with asphalt by immersing it in an asphalt–toluene solution and dried via natural drying route [104]. The author discussed that functional groups such as alkyl, sulfur and nitrogen were separated from the aromatic ring structure as the temperature reached around 400 °C via cracking and began to aggregate and formed graphene at around 600 °C. Nonetheless, it was later found by the authors that 940 °C is the optimum temperature to get a good quality multilayer 3D graphene. Figure 8 shows the possible growth mechanism of graphene from asphalt. Unlike mechanism related to aromatic compound precursors, asphalt seems to require higher energy to promote graphene growth. This can be explained by the complexity and the viscous nature of asphalt.

Unzipping nanotubes

Rolling a sheet of graphene would create a CNT. The stacking of significant amount of graphene would create graphite while if the right size of graphene is crumpled into a ball, fullerene will be produced [145]. Therefore, by reverse engineering the process, the

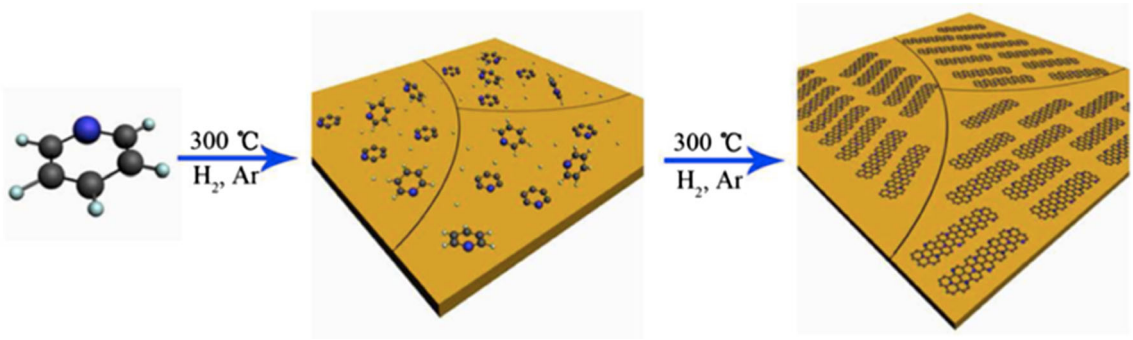

Figure 6 Schematic of nitrogen-doped graphene synthesis on a Cu surface with pyridine as carbon source (gray atoms = C atoms, light green atoms = H atoms, blue atoms = N atoms). Reprinted with permission from [94].

graphite, fullerene and CNT can be converted into its fundamental structure, which is graphene. In fact, that is how graphene was discovered in the first place in 2004. Using mechanical exfoliation or scotch tape method, graphite is broken down until graphene flakes can be found [146]. The same can be said hypothetically about CNT. If the CNT is 'cut' in a way that allows the tube to be unzipped, the CNT can be transformed into graphene. Yan et al. [122] were successful in producing rebar graphene (for 'reinforced bar graphene') by using functionalized CNTs as the starting material. As shown in Fig. 9, single-wall CNTs (SWCNTs) were partially unzipped due to the etching mechanism applied at high temperature with the presence of Cu foil as catalyst. The edges of the unzipped SWCNTs could capture active carbon species to continue the growth of graphene [147]. The exposed hexagonal rings covalently bond graphene islands and the unzipped SWCNTs together. As a result, the graphene formed has additional

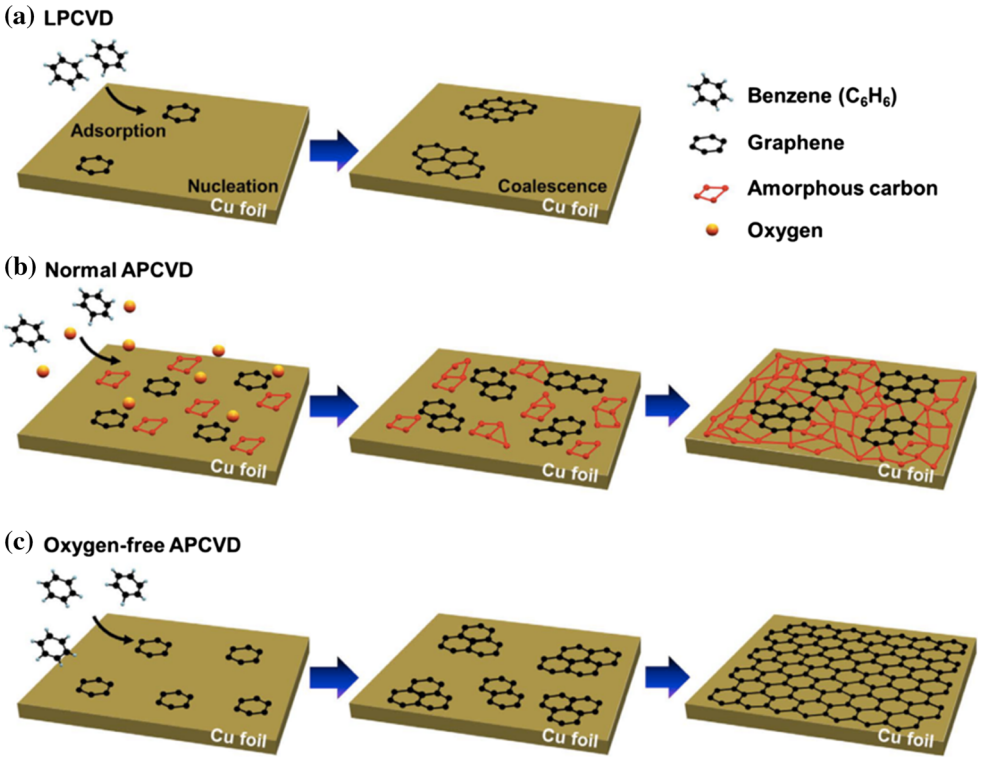

Figure 7 Schematic diagram of growth mechanism on a Cu surface from benzene by **a** LPCVD; **b** normal APCVD; **c** oxygen-free APCVD. Reprinted with permission from [49].

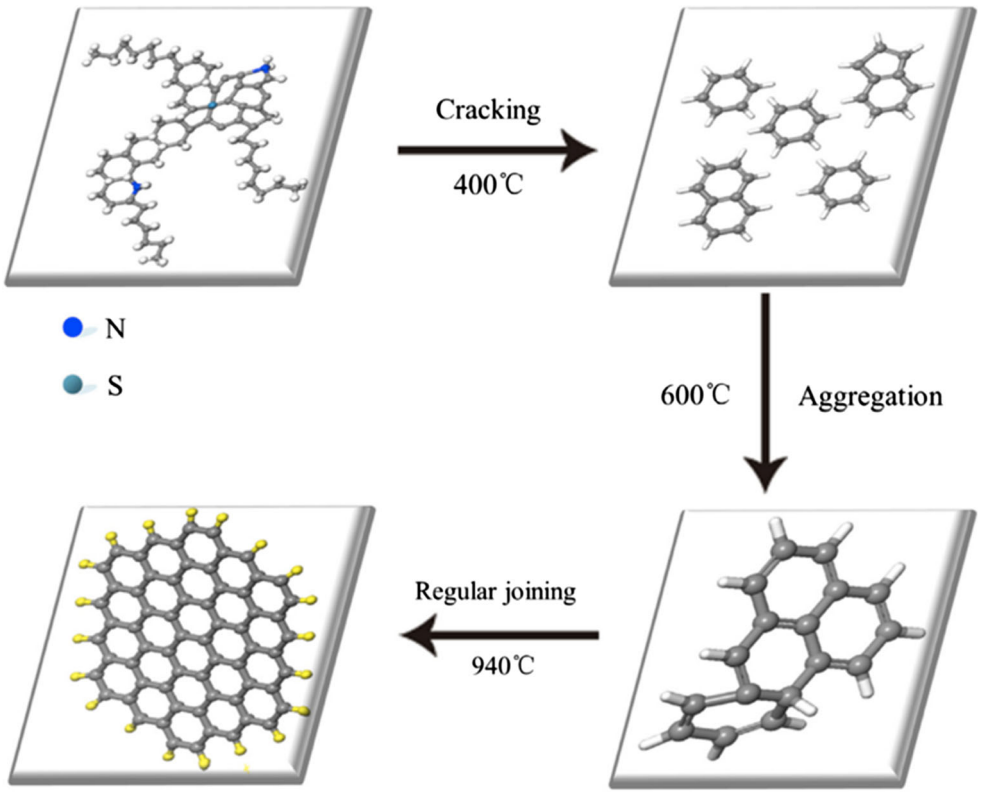

Figure 8 Possible growth mechanism of 3D graphene CVD from asphalt. Reprinted with permission from [104].

π–π-stacked graphene–SWCNT interfaces that ensues a tougher graphene arrangement. This has been fittingly named as the unzipping CNT mechanism.

The first time that freestanding rebar graphene was reported, functionalized CNTs on Cu foil were annealed without needing to introduce extraneous carbon precursor. However, recent research by Sha et al. [148] has taken a different approach in utilizing carbon nanotube unzipping mechanism. Here, freestanding three-dimensional (3D) rebar graphene foam was developed by using multiwall CNT (MWCNT) as a reinforcing bar and sucrose as the solid carbon source. A simple powder metallurgy template method was used combined with sintered Ni skeletons as a template for CVD growth. The MWCNT works as π–π-stacked bridges between carbon shell structures and graphene, which resulted in a 3D rebar graphene foam with higher strength, structural stability, storage modulus, thermal stability and conductivity. Aside from CNTs, other forms of nanotubes such as functionalized boron nitride nanotubes (BNNTs) have also been used in the past to enhance the mechanical strength of the primary graphene through covalent bonds. Li et al. [149] report that the BNNTs also partially unzip and form a reinforcing bar network. The solid carbon source used for the primary graphene growth was the wrapped Pluronic 127 surfactant.

Other carbon precursors

There are a few carbon precursors that do not fit with any of the mentioned pathways. Camphor which is comprised of pentagonal and hexagonal rings attached to methyl carbon falls under this category [113]. The carbon rings present within camphor can diffuse on the metal substrate directly without any intervention to form large-area graphene. Camphor chemical composition is quite complex since it contains abundant oxygen and hydrogen atoms. The presence of these two elements actually permits a good coordination between the metal substrate used and assists graphene formation. Most importantly, substrate preferential diffusion and reduction in the

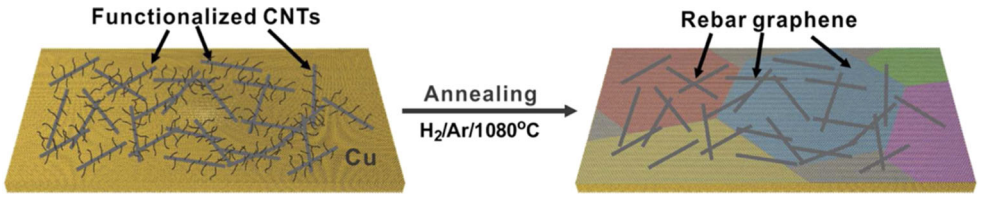

Figure 9 Scheme of rebar graphene synthesis on Cu foil from CNTs. Reprinted with permission from [122].

carbon dissolution are key factors in graphene CVD of monolayer graphene [150]. Figure 10 shows the schematic diagram of graphene CVD pathway as camphor is used as carbon precursor.

Certain precursors are just too complex and composed of various chemical compounds that it becomes very hard to precisely determine the involved mechanism. In the past, a few researchers have successfully synthesized graphene from flower petals [99], grass, cockroach leg and dog feces [98]. All of the said carbon precursors are living organisms or at least produced from living organisms. Cookies and chocolate are used as well as carbon precursors for successful graphene growth without the true nature of the involved mechanisms known.

Besides that, amorphous carbon has also been used as carbon feedstock for graphene growth [119, 120]. However, graphene could only be synthesized if H_2 was present in the CVD reaction chamber. It was suggested that the amorphous carbon film reacted with H_2 and ultimately yielded graphene on the Cu foil. The CVD process also needed to be run at elevated temperature to grow graphene. After all, amorphous carbon does not have the unique feature of aromatic compounds or CNTs. The elevated temperature is compulsory to provide the energy to break down amorphous carbon structure to form active carbon species that next coalesce with other carbon species to form graphene. Plus, unlike rebar graphene, the graphene synthesized using amorphous carbon does not seem to have any advantages compared to that formed from other carbon precursors.

As a summary, there are a few distinctive observable mechanisms for carbon precursors in graphene CVD as illustrated in Table 5. CNTs stand as the unique case in the field because of the feasible unzipping mechanism. Other than that, low-temperature CVD to produce high-quality graphene by using aromatic compounds is becoming of great importance in graphene synthesis field. Unlike the other carbon precursors, it was suggested that aromatic compounds have C_6 hexagonal ring intermediates as the active species [89]. This occurrence allows graphene formation on the metal substrate at lower-temperature region than if a straight-chain hydrocarbon is used. However, it depends on whether the dehydrogenation temperature is lower than the pyrolysis temperature of the compound itself. So, the mechanism also depends heavily on the conditions of the CVD reaction. The formation of graphene from carbon active species seems to be endothermic and requires higher amount of energy than C_6 hexagonal ring active species and hence the higher reaction temperature. Aromatic compound precursors on the other hand skip the process in question as they already have a C_6 hexagonal ring as illustrated in Fig. 11, resulting in a lower reaction temperature for graphene growth. This finding can have a profound effect in the graphene community as it solves the longtime issue of high-temperature reaction to produce graphene. Currently, plasma is heavily studied as a solution to this issue.

Future prospects

At the moment, many carbon source materials have been tested and they prove to be able to grow graphene. The expertise and knowledge regarding

Figure 10 Suggested graphene CVD scheme with camphor as carbon precursor. Reprinted with permission from [150].

Table 5 Observable mechanisms from various carbon precursors for graphene growth by CVD

Mechanism groups	Carbon precursors	Graphene growth reaction mechanism			
		Step 1	Step 2	Step 3	Step 4
Aliphatic compound mechanism	Methane [68], acetylene [72], ethylene [74], propene [78], pentane [87], hexane [83], fluorine [102], methanol, ethanol [84], propanol [82], PMMA [56], acrylonitrile butadiene styrene [106], sucrose [102]	Partial of full dehydrogenation, denitrogenation, deoxygenation into carbon active species	Carbon active species deposit on metal substrate and formed into sp^2 formation graphene nuclei	Graphene edges capture active carbon for graphene growth	Graphene islands bonded with other graphene islands to form larger graphene
Aromatic compound mechanism	Benzene [49], pyridine [140], *p*-terphenyl [89], hexachlorobenzene [124]	Partial of full dehydrogenation, denitrogenation, deoxygenation into active aromatic ring active species		Aromatic ring active species deposit onto metal substrate, capture active carbon for graphene growth and become graphene nuclei	Graphene islands bonded with other graphene islands to form larger graphene
Unzipping nanotube mechanism	Carbon nanotube [122], boron nitride nanotube [149]	Nanotube bond partially unzipped	Primary graphene surface and unzipped nanotube edges capture active carbon for graphene growth	Graphene and nanotube covalently bonded together by aromatic rings in the partially unzipped CNT region	

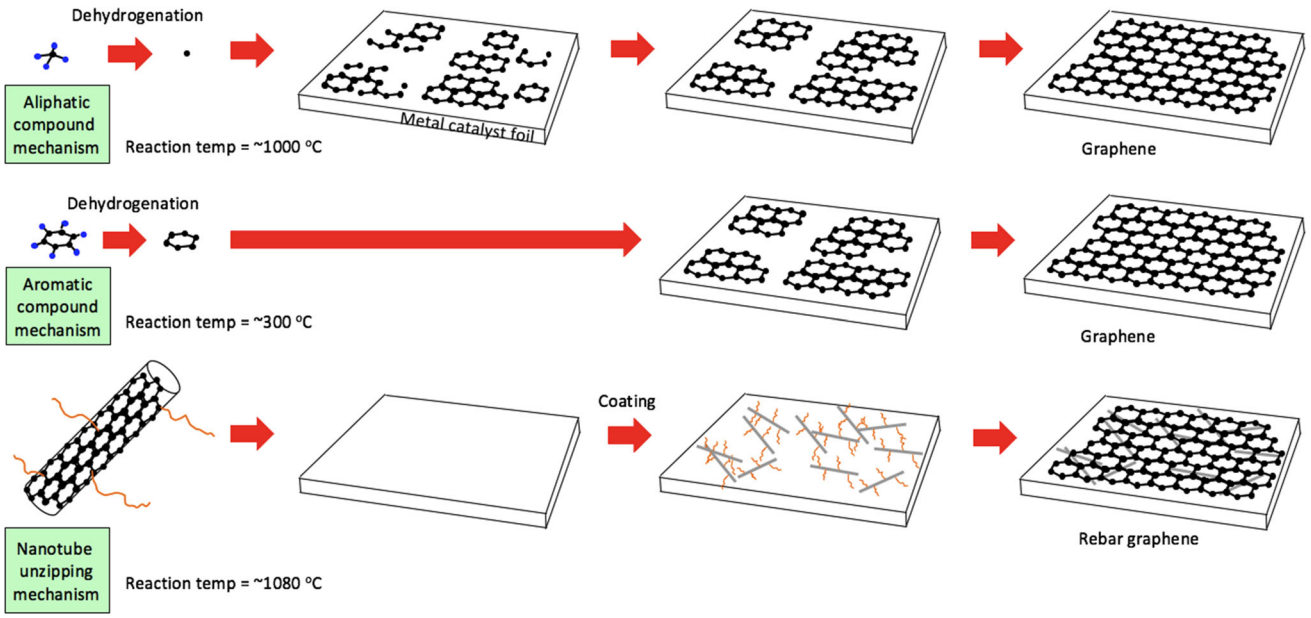

Figure 11 Graphical illustration of observable mechanisms from various carbon precursors for graphene growth by CVD. Adapted from [49, 122].

carbon precursors for graphene synthesis by CVD still has a long way to go. There are a number of issues and challenges that need to be continually investigated for the synthesis of graphene via the CVD method:

(a) The use of suitable carbon precursor with the right conditions can improve the production cost. Aromatic compounds epitomize the simplicity of solving the major stumbling block for graphene commercialization. If a similar setup were used for benzene and methane, the graphene growth reaction temperature used for benzene would be significantly lower than that used for methane, reducing the amount of energy, lead time and cost of the overall process. However, aromatic compounds are well known to be carcinogenic in nature. Hence, the safety aspect of the production setup needs to be in top-notch condition. This issue is something that can be solved with continuous effort of research. After all, there are a lot of chemical processes which involved the use of hazardous materials.

(b) Another issue is regarding the transport of carbon precursor through the reaction chamber. A two-furnace setup for graphene synthesis required while using liquid and solid carbon precursors are not an ideal setup as it reduces the efficiency of the process considering the length of the quartz tube that is longer to accommodate the extra furnace. Some researchers have proposed the use of spray CVD for liquid precursors. Though, this method requires an extremely high-precision spray mechanism considering the amount of carbon precursor required for graphene growth since 1 atom thick is considerably low. Not to mention the gas that will be used as the external force needs to be inert and not react chemically once it has gone inside the reaction chamber. A more innovative solution is required so that graphene can reach its full potential as the next-generation material of the future.

(c) Recently, new techniques of graphene synthesis besides CVD have been reported. Laser ablation-induced transformation of graphite into graphene [151], electrochemical exfoliation [152–155] and plasma-enhanced arc discharge [156] are some of the most popular new techniques for graphene synthesis. Is it the sign of CVD is getting less popular? On the contrary, the rise of new techniques other than CVD seems to stem from the saturation of CVD research and development. CVD has been explored for quite some time now. In fact, there are already few papers that have investigated

the feasibility of large-scale production of graphene via CVD [32, 157]. Development of new techniques allows identifying their advantages and disadvantages compared to CVD, and this is the whole graphene production area that makes progress. In the end, the best graphene synthesis method would probably be a combination of these new techniques with CVD.

(d) The research in this field is somehow overlooked as most researchers are concentrating efforts on research areas such as plasma etching [158], laser ablation, catalyst modification and electrochemical bubbling for graphene transfer. The research regarding carbon precursors for graphene growth by CVD might seems simple, but their impact on the graphene growth is not negligible. Recent study has shown that oxygen-free APCVD using benzene as carbon precursor can grow graphene ($\sim 1\ cm^2$) at 300 °C with a surface coverage of 100%, a field-effect mobility of 1900–2500 $cm^2/V/s$ and an optical transmittance of 97.6% [49]. This result is remarkably better than most graphene produced by plasma-assisted CVD, which are normally damaged by the bombardment of the plasma energy. Moreover, plasma-enhanced CVD incurs some cost increase due to the energy that it consumes. Unlike PECVD, natural carbon precursors are available in abundance and a cheaper solution in every sense.

Summary

Graphene is a super material with extraordinary properties that can be the catalyst for the evolution of the next-generation devices, and CVD seems to be the most prominent production route for large-scale production of graphene. After an extensive and comprehensive investigation on various carbon precursors used to grow graphene, it appears that the state (liquid, solid and gas) of the carbon precursor does not fully correlate with the graphene growth conditions. Instead, the chemical structure of the precursor seems to play the vital role in determining the graphene synthesis. In particular, aromatic compounds for which the structure is similar to the fundamental network of graphene appear as interesting precursors. In this review, three different graphene growth mechanisms were proposed based on the chemical family of the carbon precursor used: (a) aliphatic compounds; (b) aromatic compounds; (c) unzipping nanotubes. Such approach quite well explains why the CVD graphene growth temperature from aromatic compounds is really low compared to that observed with aliphatic compounds. Conceivably, this can be a part of the solution for low-cost graphene synthesis. However, more studies that are more thorough need to be performed so that precise control of graphene growth can be achieved.

Acknowledgements

The authors gratefully acknowledge the financial support provided by the Government of Malaysia (MyBrain), USM-NanoMITE (203/PJKIMIA/6720009) and Fundamental Research Grant Scheme (203/PJKIMIA/6071335).

References

[1] Gilje S, Han S, Wang M et al (2007) A chemical route to graphene for device applications. Nano Lett 7:3394–3398

[2] Ahmad I, Islam M, Abdo HS et al (2015) Toughening mechanisms and mechanical properties of graphene nanosheet-reinforced alumina. Mater Des 88:1234–1243

[3] Wang F, Drzal LT, Qin Y, Huang Z (2014) Mechanical properties and thermal conductivity of graphene nanoplatelet/epoxy composites. J Mater Sci 50:1082–1093. doi:10.1007/s10853-014-8665-6

[4] Gadipelli S, Guo ZX (2015) Graphene-based materials: synthesis and gas sorption, storage and separation. Prog Mater Sci 69:1–60

[5] Huang X, Qi X, Boey F, Zhang H (2012) Graphene-based composites. Chem Soc Rev 41:666–686

[6] Wang T, Tsai J (2016) Investigating thermal conductivities of functionalized graphene and graphene/epoxy nanocomposites. Comput Mater Sci 122:272–280

[7] Wang X, Li J, Wang Y (2016) Improved high temperature strength of copper–graphene composite material. Mater Lett 181:309–312

[8] Geim AK (2009) Graphene: status and prospects. Science 324:1530

[9] Zhu S, Yuan S, Janssen GCAM (2014) Optical transmittance of multilayer graphene. Lett J Explor Front Phys 108:17007

[10] Weber JW, Bol AA, Van De Sanden MCM (2014) An improved thin film approximation to accurately determine the optical conductivity of graphene from infrared transmittance. Appl Phys Lett 105:13105

[11] Pang J, Bachmatiuk A, Ibrahim I et al (2016) CVD growth of 1D and 2D sp^2 carbon nanomaterials. J Mater Sci 51:640–667. doi:10.1007/s10853-015-9440-z

[12] Lee HC, Liu W-W, Chai S-P et al (2017) Review of the synthesis, transfer, characterization and growth mechanisms of single and multilayer graphene. RSC Adv 7:15644–15693

[13] Casaluci S, Gemmi M, Pellegrini V et al (2016) Graphene-based large area dye-sensitized solar cell modules. Nanoscale 8:5368–5378

[14] Mittal G, Dhand V, Rhee KY et al (2015) A review on carbon nanotubes and graphene as fillers in reinforced polymer nanocomposites. J Ind Eng Chem 21:11–25

[15] Young RJ, Kinloch IA, Gong L, Novoselov KS (2012) The mechanics of graphene nanocomposites: a review. Compos Sci Technol 72:1459–1476

[16] Kumar R, Singh RK, Singh AK et al (2017) Facile and single step synthesis of three dimensional reduced graphene oxide-$NiCoO_2$ composite using microwave for enhanced electron field emission properties. Appl Surf Sci 416:259–265

[17] Ke Q, Wang J (2016) Graphene-based materials for supercapacitor electrodes—a review. J Mater 2:37–54

[18] Kumar R, Joanni E, Singh RK et al (2017) Direct laser writing of micro-supercapacitors on thick graphite oxide films and their electrochemical properties in different liquid inorganic electrolytes. J Colloid Interface Sci 507:271–278

[19] Kumar R, Singh RK, Vaz AR et al (2017) Self-assembled and one-step synthesis of interconnected 3D network of Fe_3O_4/reduced graphene oxide nanosheets hybrid for high-performance supercapacitor electrode. ACS Appl Mater Interfaces 9:8880–8890

[20] Kucinskis G, Bajars G, Kleperis J (2013) Graphene in lithium ion battery cathode materials: a review. J Power Sources 240:66–79

[21] Zhao L, Li H, Li M et al (2016) Lithium-ion storage capacitors achieved by CVD graphene/TaC/Ta-wires and carbon hollow spheres. Appl Energy 162:197–206

[22] Kheirabadi N, Shafiekhani A (2012) Graphene/Li-ion battery. J Appl Phys 112:124323

[23] Devrim Y, Albostan A (2016) Graphene-supported platinum catalyst-based membrane electrode assembly for PEM fuel cell. J Electron Mater 45:3900–3907

[24] Najafabadi AT, Leeuwner MJ, Wilkinson DP, Gyenge EL (2016) Electrochemically produced graphene for microporous layers in fuel cells. Chemsuschem 9:1–10

[25] Kuhn L, Gorji NE (2016) Review on the graphene/nanotube application in thin film solar cells. Mater Lett 171:323–326

[26] Putri LK, Ong WJ, Chang WS, Chai SP (2015) Heteroatom doped graphene in photocatalysis: a review. Appl Surf Sci 358:2–14

[27] Park CS, Yoon H, Kwon OS (2016) Graphene-based nanoelectronic biosensors. J Ind Eng Chem 38:13–22

[28] Zhao Y, Li X, Zhou X, Zhang Y (2016) Review on the graphene based optical fiber chemical and biological sensors. Sens Actuators B Chem 231:324–340

[29] Aghigh A, Alizadeh V, Wong HY et al (2015) Recent advances in utilization of graphene for filtration and desalination of water: a review. Desalination 365:389–397

[30] Jin Z, Owour P, Lei S, Ge L (2015) Graphene, graphene quantum dots and their applications in optoelectronics. Curr Opin Colloid Interface Sci 20:439–453

[31] Polat EO, Uzlu HB, Balci O et al (2016) Graphene-enabled optoelectronics on paper. ACS Photonics 3:964–971

[32] Bae S, Kim H, Lee Y et al (2010) Roll-to-roll production of 30-inch graphene films for transparent electrodes. Nat Nanotechnol 5:574–578

[33] Levchenko I, Ostrikov K, Zheng J et al (2016) Scalable graphene production: perspectives and challenges of plasma applications. Nanoscale 8:10511–10527

[34] Seah C-M, Chai S-P, Mohamed AR (2014) Mechanisms of graphene growth by chemical vapour deposition on transition metals. Carbon 70:1–21

[35] Geim AK, Novoselov KS (2007) The rise of graphene. Nat Mater 6:183–191

[36] Botas C, Alvarez P, Blanco P et al (2013) Graphene materials with different structures prepared from the same graphite by the Hummers and Brodie methods. Carbon 65:156–164

[37] Muhammad S, Ritikos R, James T et al (2014) A practical carbon dioxide gas sensor using room-temperature hydrogen plasma reduced graphene oxide. Sens Actuators B Chem 193:692–700

[38] Li X, Zhang G, Bai X et al (2008) Highly conducting graphene sheets and Langmuir–Blodgett films. Nat Nanotechnol 3:538–542

[39] Robinson J, Weng X, Trumbull K et al (2010) Nucleation of epitaxial graphene on SiC(0001). ACS Nano 4:153–158

[40] Sun J, Chen Y, Priydarshi MK et al (2015) Direct chemical vapor deposition-derived graphene glasses targeting wide ranged applications. Nano Lett 15:5846–5854

[41] Choucair M, Thordarson P, Stride JA (2009) Gram-scale production of graphene based on solvothermal synthesis and sonication. Nat Nanotechnol 4:30–33

[42] Wang G, Zhang M, Zhu Y et al (2013) Direct growth of graphene film on germanium substrate. Sci Rep 3:1–6
[43] Weatherup RS, Shahani AJ, Wang ZJ et al (2016) In situ graphene growth dynamics on polycrystalline catalyst foils. Nano Lett 16:6196–6206
[44] De Volder MFL, Tawfick SH, Baughman RH, Hart AJ (2013) Carbon nanotubes: present and future commercial applications. Science 339:535–539
[45] Batzill M (2012) The surface science of graphene: metal interfaces, CVD synthesis, nanoribbons, chemical modifications, and defects. Surf Sci Rep 67:83–115
[46] Sun H, Xu J, Wang C et al (2016) Synthesis of large-area monolayer and bilayer graphene using solid coronene by chemical vapor deposition. Carbon 108:356–362
[47] Braeuninger-Weimer P, Brennan B, Pollard AJ, Hofmann S (2016) Understanding and controlling Cu-catalyzed graphene nucleation: the role of impurities, roughness, and oxygen scavenging. Chem Mater 28:8905–8915
[48] Seah CM, Vigolo B, Chai SP et al (2016) Sequential synthesis of free-standing high quality bilayer graphene from recycled nickel foil. Carbon 96:268–275
[49] Jang J, Son M, Chung S et al (2015) Low-temperature-grown continuous graphene films from benzene by chemical vapor deposition at ambient pressure. Sci Rep 5:17955
[50] Lee K, Ye J (2016) Significantly improved thickness uniformity of graphene monolayers grown by chemical vapor deposition by texture and morphology control of the copper foil substrate. Carbon 100:441–449
[51] Kato R, Minami S, Koga Y, Hasegawa M (2016) High growth rate chemical vapor deposition of graphene under low pressure by RF plasma assistance. Carbon 96:1008–1013
[52] Fang L, Yuan W, Wang B, Xiong Y (2016) Growth of graphene on Cu foils by microwave plasma chemical vapor deposition: the effect of in situ hydrogen plasma post-treatment. Appl Surf Sci 383:28–32
[53] Li X, Cai W, An J et al (2009) Large area synthesis of high quality and uniform graphene films on copper foils. Science 324:1312–1314
[54] Suk JW, Kitt A, Magnuson CW et al (2011) Transfer of CVD-grown monolayer graphene onto arbitrary substrates. ACS Nano 5:6916–6924
[55] Li X, Cai W, Colombo L, Ruoff RS (2009) Evolution of graphene growth on Ni and Cu by carbon isotope labeling. Nano Lett 9:4268–4272
[56] Li Z, Wu P, Wang C et al (2011) Low-temperature growth of graphene by chemical vapor deposition using solid and liquid carbon sources. ACS Nano 5:3385–3390
[57] Suriani AB, Dalila AR, Mohamed A et al (2015) Synthesis of carbon nanofibres from waste chicken fat for field electron emission applications. Mater Res Bull 70:524–529
[58] Ouyang B, Jacob MV, Rawat RS (2015) Free standing 3D graphene nano-mesh synthesis by RF plasma CVD using non-synthetic precursor. Mater Res Bull 71:61–66
[59] Rosmi MS, Shinde SM, Rahman NDA et al (2016) Synthesis of uniform monolayer graphene on re-solidified copper from waste chicken fat by low pressure chemical vapor deposition. Mater Res Bull 83:573–580
[60] Liu H, Kishi N, Soga T (2015) Synthesis of thiolated few-layered graphene by thermal chemical vapor deposition using solid precursor. Mater Lett 159:114–117
[61] Somani PR, Somani SP, Umeno M (2006) Planer nano-graphenes from camphor by CVD. Chem Phys Lett 430:56–59
[62] Au C-T, Ng C-F, Liao M-S (1999) Methane dissociation and syngas formation on Ru, Os, Rh, Ir, Pd, Pt, Cu, Ag, and Au: a theoretical study. J Catal 185:12–22
[63] An W, Zeng XC, Turner CH (2009) First-principles study of methane dehydrogenation on a bimetallic Cu/Ni(111) surface. J Chem Phys 131:174702
[64] Kordatos A, Kelaidis N, Giamini SA et al (2016) AB stacked few layer graphene growth by chemical vapor deposition on single crystal Rh(111) and electronic structure characterization. Appl Surf Sci 369:251–256
[65] Reina A, Jia X, Ho J et al (2009) Large area, few-layer graphene films on arbitrary substrates by chemical vapor deposition. Nano Lett 9:30–35
[66] Guo W, Xu C, Xu K et al (2015) Rapid chemical vapor deposition of graphene on liquid copper. Synth Met 216:93–97
[67] Pollard AJ (2015) Metrology for graphene and 2-D materials. In: 17 th international congress of metrology, vol 1, pp 1–7
[68] Yang M, Sasaki S, Suzuki K, Miura H (2016) Control of the nucleation and quality of graphene grown by low-pressure chemical vapor deposition with acetylene. Appl Surf Sci 366:219–226
[69] Gottardi S, Müller K, Bignardi L et al (2015) Comparing graphene growth on Cu(111) versus oxidized Cu(111). Nano Lett 15:917–922
[70] Reckinger N, Van Hooijdonk E, Joucken F et al (2014) Anomalous moiré pattern of graphene investigated by scanning tunneling microscopy: evidence of graphene growth on oxidized Cu (111). Nano Res 7:154–162
[71] Chen CS, Hsieh CK (2015) Effects of acetylene flow rate and processing temperature on graphene films grown by thermal chemical vapor deposition. Thin Solid Films 584:265–269
[72] Mueller NS, Morfa AJ, Abou-Ras D et al (2014) Growing graphene on polycrystalline copper foils by ultra-high vacuum chemical vapor deposition. Carbon 78:347–355

[73] Qi M, Ren Z, Jiao Y et al (2013) Hydrogen kinetics on scalable graphene growth by atmospheric pressure chemical vapor deposition with acetylene. J Phys Chem C 117:14348–14353

[74] Trinsoutrot P, Vergnes H, Caussat B (2014) Three dimensional graphene synthesis on nickel foam by chemical vapor deposition from ethylene. Mater Sci Eng B Solid State Mater Adv Technol 179:12–16

[75] Celebi K, Cole MT, Teo KBK, Park HG (2011) Observations of early stage graphene growth on copper. Electrochem Solid State Lett 15:K1–K4

[76] Addou R, Dahal A, Sutter P, Batzill M (2012) Monolayer graphene growth on Ni(111) by low temperature chemical vapor deposition. Appl Phys Lett 100:10–13

[77] Sagar RR, Zhang X, Xiong C (2014) Growth of graphene on copper and nickel foils via chemical vapour deposition using ethylene. Mater Res Innovations 18:S4706–S4710

[78] Gotterbarm K, Zhao W, Höfert O et al (2013) Growth and oxidation of graphene on Rh(111). Phys Chem Chem Phys 15:19625

[79] Liu W-W, Chai S-P, Mohamed AR, Hashim U (2014) Synthesis and characterization of graphene and carbon nanotubes: a review on the past and recent developments. J Ind Eng Chem 20:1171–1185

[80] Strudwick AJ, Weber NE, Schwab MG et al (2015) Chemical vapor deposition of high quality graphene films from carbon dioxide atmospheres. ACS Nano 9:31–42

[81] Yagi K, Yamada A, Hayashi K et al (2013) Dependence of field-effect mobility of graphene grown by thermal chemical vapor deposition on its grain size. Jpn J Appl Phys 52:110106

[82] Guermoune A, Chari T, Popescu F et al (2011) Chemical vapor deposition synthesis of graphene on copper with methanol, ethanol, and propanol precursors. Carbon 49:4204–4210

[83] Srivastava A, Galande C, Ci L et al (2010) Novel liquid precursor-based facile synthesis of large-area continuous, single, and few-layer graphene films. Chem Mater 22:3457–3461

[84] Miyata Y, Kamon K, Ohashi K (2010) A simple alcohol-chemical vapor deposition synthesis of single-layer graphenes using flash cooling. Appl Phys Lett 96:263105

[85] Kishi N, Fukaya A, Sugita R et al (2012) Synthesis of graphenes on Ni foils by chemical vapor deposition of alcohol with IR-lamp heating. Mater Lett 79:21–24

[86] Pollard AJ, Brennan B, Stec H et al (2014) Quantitative characterization of defect size in graphene using Raman spectroscopy. Appl Phys Lett 105:253107

[87] Dong X, Wang P, Fang W et al (2011) Growth of large-sized graphene thin-films by liquid precursor-based chemical vapor deposition under atmospheric pressure. Carbon 49:3672–3678

[88] John R, Ashokreddy A, Vijayan C, Pradeep T (2011) Single- and few-layer graphene growth on stainless steel substrates by direct thermal chemical vapor deposition. Nanotechnology 22:165701

[89] Choi J-H, Li Z, Cui P et al (2013) Drastic reduction in the growth temperature of graphene on copper via enhanced London dispersion force. Sci Rep 3:1925

[90] Seo DH, Pineda S, Fang J et al (2017) Single-step ambient-air synthesis of graphene from renewable precursors as electrochemical genosensor. Nat Commun 8:14217

[91] Salifairus MJ, Abd Hamid SB, Soga T et al (2016) Structural and optical properties of graphene from green carbon source via thermal chemical vapor deposition. J Mater Res 31:1–10

[92] Jalani D, Rahman SFA, Hashim AM (2016) Defect-free mixed mono- and bi-layer graphene synthesized from refined palm oil by thermal chemical vapor deposition. Mater Lett 182:168–172

[93] Han Q, Shan H, Deng J et al (2014) Construction of carbon-based two-dimensional crystalline nanostructure by chemical vapor deposition of benzene on Cu(111). Nanoscale 6:7934–7939

[94] Xue Y, Wu B, Jiang L et al (2012) Low temperature growth of highly nitrogen-doped single crystal graphene arrays by chemical vapor deposition. J Am Chem Soc 134:11060–11063

[95] Zhang C, Fu L, Liu N et al (2011) Synthesis of nitrogen-doped graphene using embedded carbon and nitrogen sources. Adv Mater 23:1020–1024

[96] Johns IB, McElhill EA, Smith JO (1962) Thermal stability of some organic compounds. J Chem Eng Data 7:277–281

[97] Gan W, Han N, Yang C et al (2017) A ternary alloy substrate to synthesize monolayer graphene with liquid carbon precursor. ACS Nano 11:1371–1379

[98] Ruan G, Sun Z, Peng Z, Tour JM (2011) Growth of graphene from food, insects, and waste. ACS Nano 5:7601–7607

[99] Ray AK, Sahu RK, Rajinikanth V et al (2012) Preparation and characterization of graphene and Ni-decorated graphene using flower petals as the precursor material. Carbon 50:4123–4129

[100] Lopez GA, Mittemeiker EJ (2004) The solubility of C in solid Cu. Scripta Mater 51:1–5

[101] Zhang Y, Zhang L, Zhou C (2013) Review of chemical vapor deposition of graphene and related applications. Acc Chem Res 46:2329–2339

[102] Sun ZZ, Yan Z, Yao J et al (2010) Growth of graphene from solid carbon sources. Nature 468:549–552

[103] Cheng IF, Xie Y, Allen Gonzales R et al (2011) Synthesis of graphene paper from pyrolyzed asphalt. Carbon 49:2852–2861

[104] Liu Z, Tu Z, Li Y et al (2014) Synthesis of three-dimensional graphene from petroleum asphalt by chemical vapor deposition. Mater Lett 122:285–288

[105] Sharma S, Kalita G, Hirano R et al (2014) Synthesis of graphene crystals from solid waste plastic by chemical vapor deposition. Carbon 72:66–73

[106] Peng Z, Yan Z, Sun Z, Tour JM (2011) Direct growth of bilayer graphene on SiO_2 substrates by carbon diffusion through nickel. ACS Nano 5:8241–8247

[107] Losurdo M, Giangregorio MM, Capezzuto P, Bruno G (2011) Graphene CVD growth on copper and nickel: role of hydrogen in kinetics and structure. Phys Chem Chem Phys 13:20836–20843

[108] Kumar M, Ando Y (2007) Carbon nanotubes from camphor: an environment-friendly nanotechnology. J Phys: Conf Ser 61:643–646

[109] Kumar M, Ando Y (2003) A simple method of producing aligned carbon nanotubes from an unconventional precursor—Camphor. Chem Phys Lett 374:521–526

[110] Kumar M, Ando Y (2003) Camphor-a botanical precursor producing garden of carbon nanotubes. Diam Relat Mater 12:998–1002

[111] Kumar M, Ando Y (2003) Single-wall and multi-wall carbon nanotubes from camphor—a botanical hydrocarbon. Diam Relat Mater 12:1845–1850

[112] Ahmed M, Kishi N, Sugita R et al (2013) Graphene synthesis by thermal chemical vapor deposition using solid precursor. J Mater Sci: Mater Electron 24:2151–2155

[113] Kalita G, Wakita K, Umeno M (2011) Monolayer graphene from a green solid precursor. Physica E 43:1490–1493

[114] Debgupta J, Mandal S, Kalita H et al (2014) Photophysical and photoconductivity properties of thiol-functionalized graphene–CdSe QD composites. RSC Adv 4:13788–13795

[115] Marquardt D, Beckert F, Pennetreau F et al (2014) Hybrid materials of platinum nanoparticles and thiol-functionalized graphene derivatives. Carbon 66:285–294

[116] Debgupta J, Pillai VK (2013) Thiolated graphene—a new platform for anchoring CdSe quantum dots for hybrid heterostructures. Nanoscale 5:3615–3619

[117] Stankovich S, Dikin DA, Dommett GHB et al (2006) Graphene-based composite materials. Nature 442:282–286

[118] Stankovich S, Dikin DA, Piner RD et al (2007) Synthesis of graphene-based nanosheets via chemical reduction of exfoliated graphite oxide. Carbon 45:1558–1565

[119] Seo JH, Lee HW, Kim J-K et al (2012) Few layer graphene synthesized by filtered vacuum arc system using solid carbon source. Curr Appl Phys 12:S131–S133

[120] Ji H, Hao Y, Ren Y et al (2011) Graphene growth using a solid carbon feedstock and hydrogen. ACS Nano 5:7656–7661

[121] Seo JH, Kang JW, Kim DH et al (2013) Simple wafer-scale growth and transfer of graphene film converted from spin-coated fullerene derivative. ECS Solid State Lett 2:M13–M16

[122] Yan Z, Peng Z, Casillas G et al (2014) Rebar graphene. ACS Nano 8:5061–5068

[123] Gan X, Zhou H, Zhu B et al (2012) A simple method to synthesize graphene at 633 K by dechlorination of hexachlorobenzene on Cu foils. Carbon 50:306–310

[124] Gao X, Wang W, Liu X (2008) Low-temperature dechlorination of hexachlorobenzene on solid supports and the pathway hypothesis. Chemosphere 71:1093–1099

[125] Barber JL, Sweetman AJ, Van Wijk D, Jones KC (2005) Hexachlorobenzene in the global environment: emissions, levels, distribution, trends and processes. Sci Total Environ 349:1–44

[126] Wong WWH, Subbiah J, Puniredd SR et al (2012) Liquid crystalline hexa-peri-hexabenzocoronene-diketopyrrolopyrrole organic dyes for photovoltaic applications. J Mater Chem 22:21131

[127] Qin L, Zhang Y, Wu X et al (2015) In situ electrochemical synthesis and deposition of discotic hexa-peri-hexabenzocoronene molecules on electrodes: self-assembled structure, redox properties, and application for supercapacitor. Small 11:3028–3034

[128] Eom D, Prezzi D, Rim KT et al (2009) Structure and electronic properties of graphene nanoislands on Co(0001). Nano Lett 9:2844–2848

[129] Mullen K, Rabe JP (2008) Nanographenes as active components of single-molecule electronics and how a scanning tunneling microscope puts them. Acc Chem Res 41:511–520

[130] Cui Y, Fu Q, Zhang H, Bao X (2011) Formation of identical-size graphene nanoclusters on Ru(0001). Chem Commun 47:1470–1472

[131] Xu M, Fujita D, Sagisaka K et al (2011) Production of extended single-layer. ACS Nano 5:1522–1528

[132] Luo Z, Lu Y, Singer DW et al (2011) Effect of substrate roughness and feedstock concentration on growth of wafer-scale graphene at atmospheric pressure. Chem Mater 23:1441–1447

[133] Liao Meng-Sheng, Chak-Tong Au, Ng Ching-Fai (1997) Methane dissociation on Ni, Pd, Pt and Cu metal (111) surfaces—a theoretical comparative study. Chem Phys Lett 272:445–452

[134] Gajewski G, Pao C-W (2011) Ab initio calculations of the reaction pathways for methane decomposition over the Cu (111) surface. J Chem Phys 135:64707

[135] Luo YR (2007) Comprehensive handbook of chemical bond energies. CRC Press, Taylor & Francis Group, Boca Baton, FL

[136] Zhang W, Wu P, Li Z, Yang J (2011) First-principles thermodynamics of graphene growth on Cu surfaces. J Phys Chem C 115:17782–17787

[137] Xiao B, Yu XF, Ding YH (2014) Theoretical investigation on the healing mechanism of divacancy defect in CNT growth by C2H2 and C2H4. J Mol Model 20:640–645

[138] Park JS, Reina A, Saito R et al (2009) G′ band Raman spectra of single, double and triple layer graphene. Carbon 47:1303–1310

[139] Ferrari AC, Meyer JC, Scardaci V et al (2006) Raman spectrum of graphene and graphene layers. Phys Rev Lett 97:1–4

[140] Jin Z, Yao J, Kittrell C, Tour JM (2011) Large-scale growth and characterizations of nitrogen-doped monolayer graphene sheets. ACS Nano 5:4112–4117

[141] Rowlinson JS (1979) The thermodynamic theory of capillarity under the hypothesis of a continuous variation of density. J Stat Phys 20:197–200

[142] Bhaviripudi S, Jia X, Dresselhaus MS, Kong J (2010) Role of kinetic factors in chemical vapor deposition synthesis of uniform large area graphene using copper catalyst. Nano Lett 10:4128–4133

[143] Son IH, Song HJ, Kwon S et al (2014) CO_2 enhanced chemical vapor deposition growth of few-layer graphene over NiOx. ACS Nano 8:9224–9232

[144] Oberlin A (1984) Carbonization and graphitization. Carbon 22:521–541

[145] Xu S, Fu H, Li Y et al (2016) Novel scroll peapod produced by spontaneous scrolling of graphene onto fullerene string. Phys Chem Chem Phys 18:10138–10143

[146] Novoselov KS, Geim AK, Morozov SV et al (2004) Electric field effect in atomically thin carbon films. Science 306:666–669

[147] Artyukhov VI, Liu Y, Yakobson BI (2012) Equilibrium at the edge and atomistic mechanisms of graphene growth. Proc Natl Acad Sci 109:15136–15140

[148] Sha J, Salvatierra RV, Dong P et al (2017) Three-dimensional rebar graphene. ACS Appl Mater Interfaces 9:7376–7384

[149] Li Y, Peng Z, Larios E et al (2015) Rebar graphene from functionalized boron nitride nanotubes. ACS Nano 9:532–538

[150] Kumar R, Singh RK, Singh DP (2016) Natural and waste hydrocarbon precursors for the synthesis of carbon based nanomaterials: graphene and CNTs. Renew Sustain Energy Rev 58:976–1006

[151] Kumar R, Singh RK, Singh DP et al (2017) Laser-assisted synthesis, reduction and micro-patterning of graphene: recent progress and applications. Coord Chem Rev 342:34–79

[152] Sharief SA, Susantyoko RA, Alhashem M, Almheiri S (2017) Synthesis of few-layer graphene-like sheets from carbon-based powders via electrochemical exfoliation, using carbon black as an example. J Mater Sci 52:11004–11013. doi:10.1007/s10853-017-1275-3

[153] Dai W, Chung CY, Alam FE et al (2017) Superior field emission performance of graphene/carbon nanofilament hybrids synthesized by electrochemical self-exfoliation. Mater Lett 205:223–225

[154] Rao KS, Senthilnathan J, Liu Y-F, Yoshimura M (2015) Role of peroxide ions in formation of graphene nanosheets by electrochemical exfoliation of graphite. Sci Rep 4:4237

[155] Wu W, Zhang C, Hou S (2017) Electrochemical exfoliation of graphene and graphene-analogous 2D nanosheets. J Mater Sci 52:10649–10660. doi:10.1007/s10853-017-1289-x

[156] Kumar R, Singh RK, Dubey PK et al (2013) Pressure-dependent synthesis of high-quality few-layer graphene by plasma-enhanced arc discharge and their thermal stability. J Nanopart Res 15:1847

[157] Polsen ES, McNerny DQ, Viswanath B et al (2015) High-speed roll-to-roll manufacturing of graphene using a concentric tube CVD reactor. Sci Rep 5:10257

[158] Mao H, Wang R, Zhong J et al (2014) Mildly O2 plasma treated CVD graphene as a promising platform for molecular sensing. Carbon 76:212–219